1.18 Triterpenes

Tetsuo Kushiro and Yutaka Ebizuka, The University of Tokyo, Tokyo, Japan

1.18.1 Introduction

Triterpenes are members of isoprenoids that are derived from a C30 precursor, squalene. Squalene itself is derived from two molecules of farnesyl diphosphate (FPP), which is the precursor of sesquiterpenes (Chapter 1.16). The unique tail-to-tail condensation of FPP is catalyzed by an enzyme squalene synthase.[1] Because of this symmetrical nature, squalene lacks diphosphate group (–OPP), and, therefore, its cyclization exclusively involves protonation (type B cyclization) to generate a carbocation, rather than an ionization, of the OPP group seen mainly in mono-, sesqui-, and diterpene biosynthesis. The majority of triterpenes found in nature are cyclic triterpenes with 1–5 ring systems. In some bacteria and protozoans, squalene is directly cyclized into pentacyclic triterpenes such as hopene by squalene:hopene cyclase (SHC). Details of this enzyme are described in Chapter 1.19. On the other hand, in animals, plants, and fungi, (3*S*)-2,3-oxidosqualene is cyclized into cyclic triterpenes by the enzyme oxidosqualene cyclase (OSC). An additional enzyme known as squalene epoxidase is required by these organisms to convert squalene into oxidosqualene, which involves a stereospecific epoxidation of the terminal olefin.[2] Because of the presence of an epoxide in oxidosqualene, all of the cyclic triterpenes derived from this precursor possess oxygen functionality at the C-3 position. These cyclic triterpenes are further converted into various metabolites including sterols, steroids, and saponins, which play an important physiological role in the cells (**Scheme 1**). Sterols and steroids are described in Chapter 1.21. Nearly 100 different skeletal types of cyclic triterpenes are known in nature, which underscores the potential ability of an OSC to produce large structural diversity from a single precursor. This chapter describes our current knowledge of this remarkable enzyme and its cyclization reaction mechanisms to generate diverse structures found in the triterpene class (**Scheme 1**).

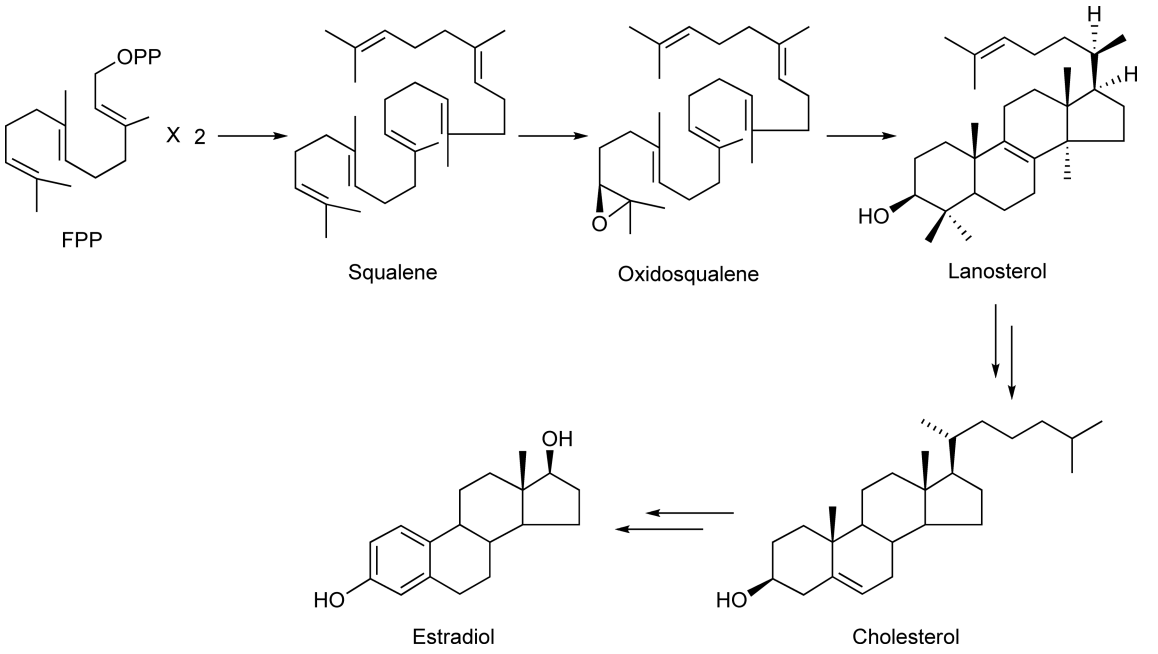

Scheme 1

1.18.2 Cyclization Mechanism

The cyclization of oxidosqualene had been a subject of intensive research over the past 60 years.[3,4] It was considered to be the most complex organic transformations found in nature, which include formation of a multiring system with numerous stereogenic centers in a single transformation. It is not just remarkable but somewhat astonishing how nature has managed to carry out such a reaction in an aqueous solution that involves reactive carbocationic intermediates. It was, thus, of prime interest to chemists how OSC handles carbocationic intermediates, controls the conformation of the substrate, and guides through the reaction sequence to produce each specific product. The OSC reaction is composed of the same basic reactions found in mono-, sesqui-, and diterpene biosynthesis; however, OSC produces up to five ring systems. The cyclization reaction of OSC can be divided into the following four parts (**Figure 1**).

1. Initiation of a reaction. A proton attack on the epoxide moiety generates an initial tertiary carbocation. The resulting OH group resides on every triterpene produced by OSC except for a few cases.
2. Propagation of a reaction through cation-π cyclization. Once formed, the carbocation undergoes attack by a nearby π electron onto an empty 2p orbital of a carbocationic center to form a C–C σ bond.
3. Further propagation through 1,2-shifts. This process is known as Wagner–Meerwein rearrangements, which include hydride, methyl, and alkyl group migration that takes place suprafacially. Ring expansion is part of this process.
4. Termination of a reaction. Deprotonation from a carbon adjacent to a carbocationic center will generate an olefin. On the other hand, a water attack onto a carbocationic center will produce a hydroxyl group.

In terms of generating triterpene structural diversity, it is important to understand how OSC exerts its huge catalytic potential to create a multitude of diverse structures. At the same time, OSC navigates the cascade of carbocation-mediated cyclization and rearrangements into particular reaction pathway to produce each specific product(s).

The catalytic potential of OSC arises primarily from the active site cavity, which is highly hydrophobic in nature and common to all of the terpene cyclase class of enzymes. Numerous hydrophobic amino acid residues compose the cavity, which binds linear isoprenoid substrates and forces them to fold into a reactive

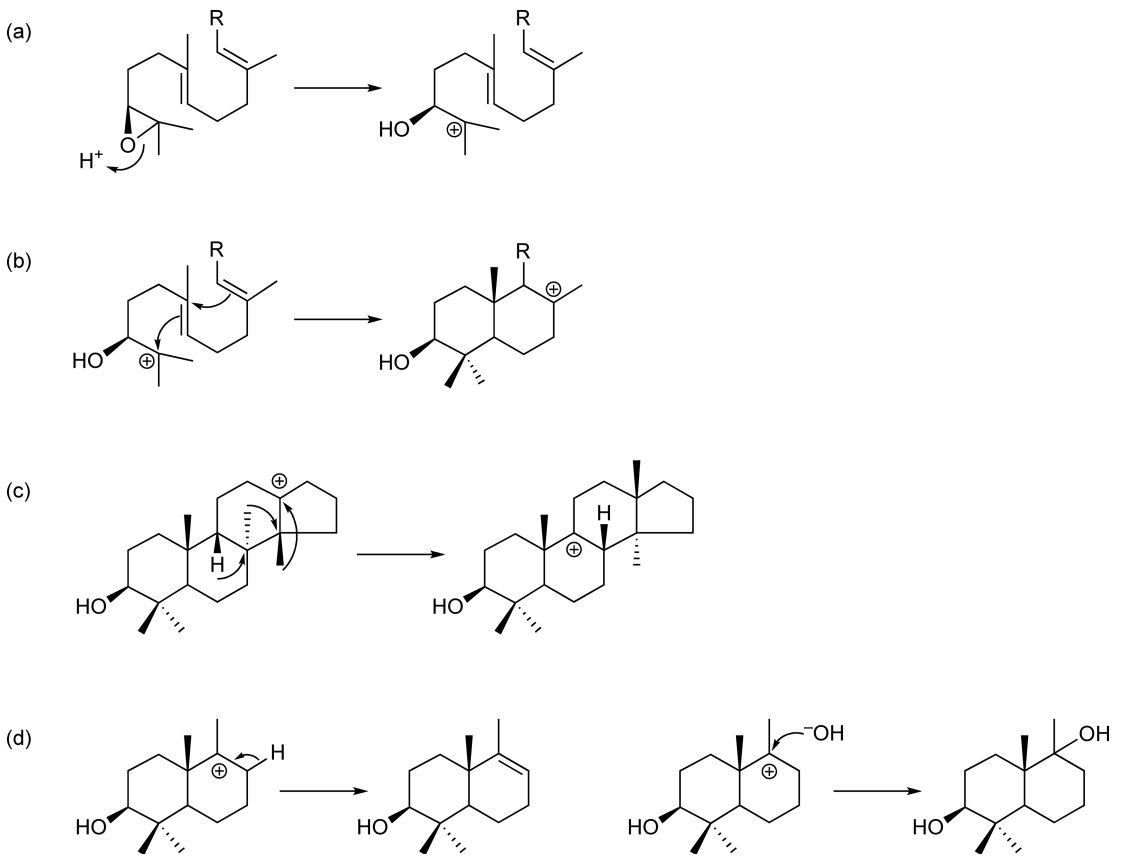

Figure 1 Four basic reactions found in OSC-catalyzed cyclization reaction.

conformation ready for cyclization cascade.[5] Steric effects are mainly responsible for the substrate folding whereas electronic effects are thought to be important for the stabilization of transition state carbocationic intermediates lowering the activation barrier to facilitate cation-π cyclization. However, calculations have suggested a rather small activation barrier for the cation-π cyclization, and there may be only a minimal assistance from the enzyme.[6] The hydrophobic cavity is also responsible for excluding solvent water molecules that may interfere with an intermediate carbocation to aberrantly quench the reaction. A strong catalytic acid is also necessary to generate a carbocation for initiation of the reaction as well as a catalytic base for terminating the reaction. The OSC reaction is highly exothermic (some 60 kcal mol^{-1} is estimated to be released during pentacyclic formation) and requires the enzyme to be rigid enough to support the protein structure during this process.

In addition, each reaction pathway leading to a particular product is determined by the number of cyclization, which dictates the number of rings formed, and by the extent to which hydride and methyl migration takes place. The number of cyclization is mainly controlled by the conformation of the substrate, that is, whether the neighboring olefin is ideally positioned for the attack of a carbocation for the next round of cyclization. The shape of the active site cavity may primarily be responsible for such a control, and, therefore, OSCs producing tetracyclic and pentacyclic structures would have different cavity shapes. In addition, stabilization of a particular carbocation may determine the lifetime of a carbocation; whether a competing reaction exists or not may also contribute to the reaction specificity. In fact, it has been considered that not only a thermodynamic control but also a kinetic control contributes to the observed product specificity.[6] That is, the reaction pathway is not determined by the relative stability of intermediate carbocationic species alone.

On the other hand, the extent of hydride and methyl migration is believed to be largely determined by the position of deprotonation. Because Wagner–Meerwein shifts can readily occur chemically in solution, there

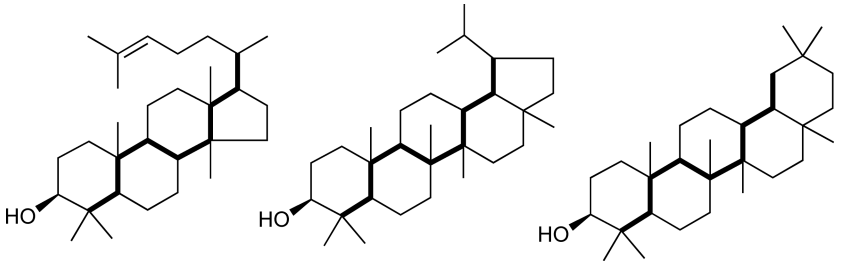

Figure 2 The path by which backbone rearrangements take place.

may be only minimal assistance from the enzyme during this process. What perhaps determines the extent of rearrangements is the position of the base (either a basic residue or a solvent water molecule) in the active site. Currently, no study has successfully identified a catalytic base among all the terpene cyclase families. The path by which these rearrangements take place on the triterpene skeleton is called *backbone rearrangement*. As depicted in **Figure 2**, in each skeletal type, rearrangements take place along the carbon atoms shown in bold lines, which gives only the tertiary carbocation during this process. Most of the products originating from each of these carbocationic centers have been identified in nature.[7]

1.18.3 Lanosterol/Cycloartenol Synthases

1.18.3.1 Mechanism

Lanosterol serves as a precursor of sterols such as cholesterol in mammals and ergosterol in yeast and fungi, whereas cycloartenol serves as a precursor of phytosterols in plants. Sterols are essential components of the cells; therefore, lanosterol synthase and cycloartenol synthase genes are essential genes in these organisms. In humans, cholesterol plays a central role in lipid physiology and is a precursor of various steroid hormones. Thus, lanosterol synthase is an ideal target for the development of clinical drugs that control cellular cholesterol levels.

Cyclization into lanosterol and cycloartenol is the most well-studied reaction among OSCs. The biosynthesis of lanosterol and cycloartenol involves oxidosqualene folded in a *chair–boat–chair* conformation in the active site. Protonation of the epoxide generates tertiary carbocation at C-2, which is then cyclized by the attack of a neighboring olefin to generate first a monocyclic carbocation **1** and then a bicyclic carbocation **2** (**Scheme 2**). Protonation triggered epoxide opening, and the first ring cyclization has been proposed to take place in a concerted manner.[8] The third ring cyclization initially forms a 6-6-5 tricyclic tertiary carbocation intermediate **3**, which then undergoes a ring expansion into six-membered C ring to form **4**. This is then followed by the fourth cyclization to give a tetracyclic intermediate, protosteryl cation **5** with a 17β side chain. From this stage, a series of Wagner–Meerwein 1,2-shifts of hydrides and methyl groups take place to give C-8 carbocation **6**, which then undergoes deprotonation from C-9 to give lanosterol (**7**) (**Scheme 2**). On the other hand, additional hydride shift from C-9 to C-8 in **6** will give C-9 carbocation **8**, which then undergoes a deprotonation from C-19 methyl group to form a cyclopropane ring of cycloartenol (**9**) (**Scheme 3**).

Initially, all of these cyclization processes were proposed to take place in a concerted manner; however, it is now generally accepted that cyclization is a stepwise process involving each discrete carbocationic intermediate. The *anti*-Markovnikov third ring cyclization was controversial for a long time because it involves an unstable secondary carbocation **4**. The existence of 6-6-5 fused intermediate **3** was suggested from the experiment using 20-oxa-2,3-oxidosqualene (**10**) as a substrate, which generated an unusual product **11** (**Scheme 4**).[9] Involvement of a ring expansion process at this stage is critical for proper formation of the 6-6-6-5 fused ring system seen in sterols. This problem arose primarily from the (oxido)squalene molecule which adopts a symmetrical structure due to tail-to-tail condensation of FPP. If it were a regular polyprenol formed through a head-to-tail condensation of isoprene units, a stable tertiary carbocation would be formed at the

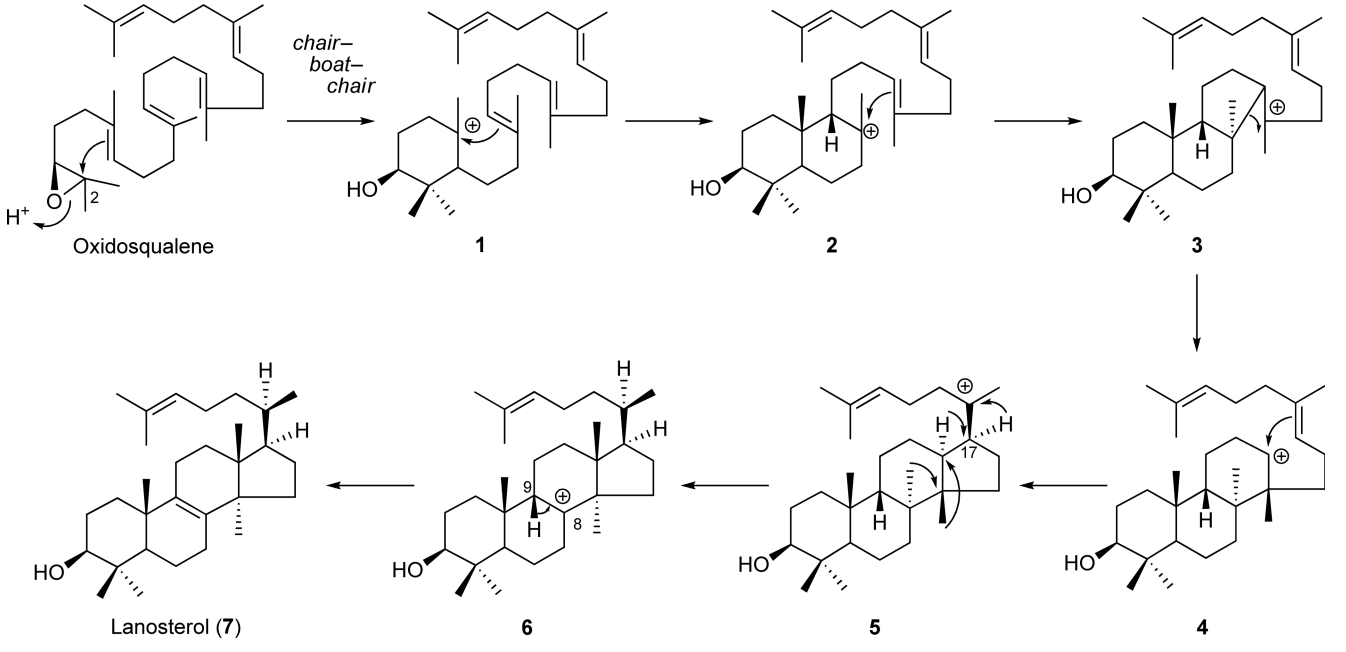

Scheme 2

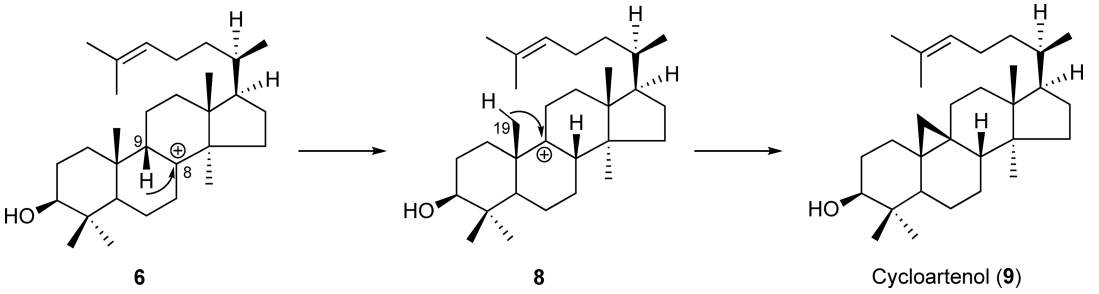

Scheme 3

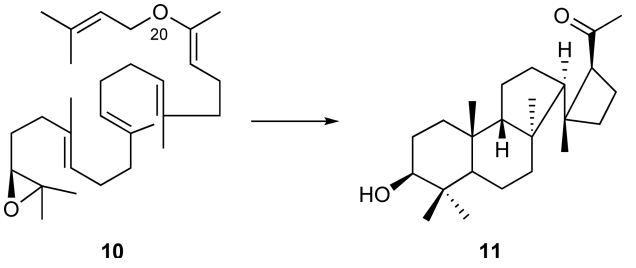

Scheme 4

tricyclic stage as exemplified in **Figure 3**. In fact, any synthetic efforts to construct a polycyclic structure from oxidosqualene using Lewis acid generate only the 6-6-5 fused tricyclic system and nothing beyond.

The stereochemistry at C-17 during protosteryl cation **5** was also a controversy in the past, as it was originally proposed to have a 17α side chain (**Figure 4(a)**); it had been proposed that the following Wagner–Meerwein hydride shift takes place in a concerted manner with strict antistereochemistry.[3] This would then require ~120° rotation of a C–C bond between C-17 and C-20 prior to hydride shift from C-17 in order to install the correct C-20*R* stereochemistry. However, incubation of **10** with yeast microsomal preparation gave a tetracyclic methyl ketone **12** with 17β configuration (**Scheme 5**).[10] This implied that **5** already had 17β side chain and oxidosqualene is folded in a conformation as shown in **Figure 4(b)**. This would require only minimum rotation of ~60° to achieve 20*R* stereochemistry prior to the hydride shift from C-17. The strict antistereochemistry during the Wagner–Meerwein shift is not always necessary.

It has been documented in the past that methyl groups of oxidosqualene play an important role in the correct folding of the substrate in the active site of the enzyme. For example, 10,15-desmethyl analogue (**13**) was shown to cyclize into an unusual product **14**, which involves a *chair–chair–boat* conformation that resulted in aberrant cyclization (**Scheme 6**).[11] Thus, methyl groups at C-10 and C-15 are important for forcing B ring into a *boat* conformation.

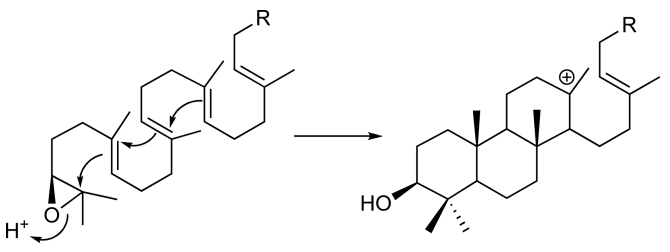

Figure 3 Hypothetical cyclization of polyprenol at tricyclic stage.

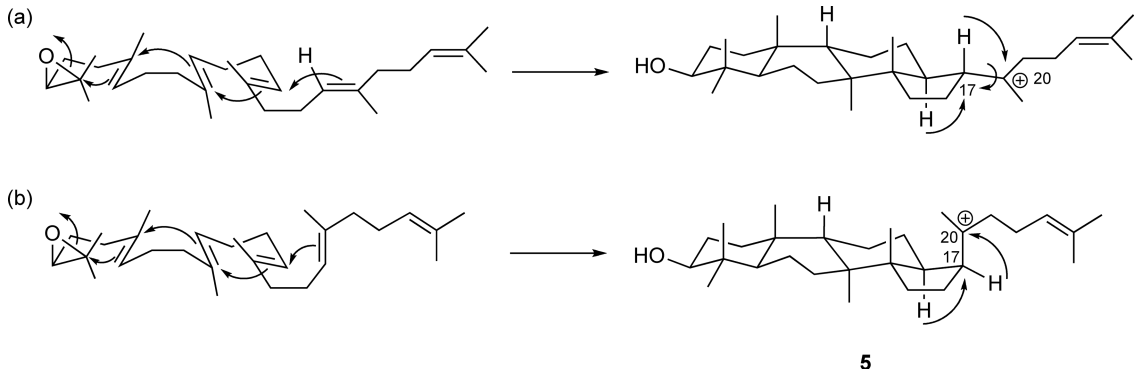

5

Figure 4 Conformation of oxidosqualene during *chair–boat–chair* cyclization to produce protosteryl cation (**5**). (a) Previously postulated conformation. (b) Currently proposed conformation.

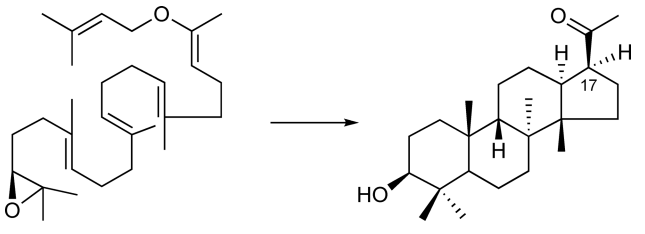

10 **12**

Scheme 5

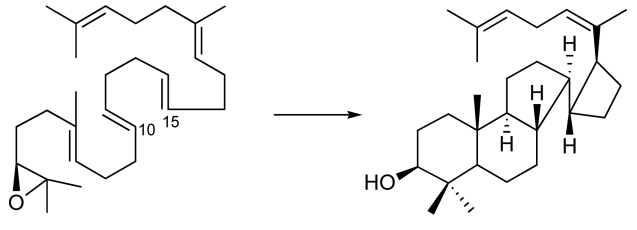

13 **14**

Scheme 6

1.18.3.2 Genes

The lanosterol synthase gene was first cloned from yeast *Candida albicans* (ERG7)[12–14] and later from *Saccharomyces cerevisiae* (ERG7),[15,16] *Schizosaccharomyces pombe*,[17] rat,[18,19] and human.[20,21] These genes code for a protein of ~730 amino acid residues with a molecular weight of ~83 kDa. Several repetitive motifs were identified and were termed QW motifs ($(K/R)(G/A)X_{2-3}(F/Y/W)(L/I/V)X_3QX_{2-5}GXW$).[22] The QW motif was also found in related bacterial SHC. It was initially thought that aromatic amino acids such as Trp in this motif might stabilize the intermediate carbocation during the cyclization reaction;[23] however, later this was proven to be wrong as these motifs were located on the surface of OSC to stabilize the protein structure.[24] Lanosterol synthase genes were further cloned from *Trypanosoma brucei*,[25] *T. cruzi*,[26] *Cephalosporium caerulens*,[27] *Pneumocystis carinii*,[28] and plants including *Arabidopsis thaliana*,[29,30] *Panax ginseng*,[30] and *Lotus japonicus*[31] (see below).

The cycloartenol synthase gene was first cloned from *A. thaliana* (AtCAS1) and found to code for a similar protein of 759 amino acid residues.[32] Sequence comparison of lanosterol and cycloartenol synthases showed 30–40% sequence identities and revealed several conserved sequences including those of QW motifs. Numerous cycloartenol synthase genes were identified later from *Pisum sativum*,[33] *P. ginseng*,[34] *Luffa cylindrica*,[35]

Dictyostelium discoideum,[36] *Glycyrrhiza glabra*,[37] *Costus speciosus*,[38] *Betula platyphylla*,[39] *Cucurbita pepo*,[40] *Ricinus communis*,[41] *L. japonicus*,[42] *Rhizophora stylosa*,[43] *Kandelia candel*,[43] and a fern, *Adiantum capillus-veneris*.[44]

Interestingly, several OSC genes have been cloned from prokaryotes as well, including lanosterol synthase from *Methylococcus capsulatus*[45,46] and cycloartenol synthase from *Stigmatella aurantiaca*.[47] Sterols are normally absent in prokaryotes, and the existence of an OSC gene in these organisms raises an intriguing question regarding the evolution of an OSC gene and a sterol biosynthesis.

1.18.3.3 Mutational Studies

Earlier on, an effort to identify the active site residues was carried out using a mechanism-based irreversible inhibitor 29-methylidene-2,3-oxidosqualene (29-MOS) (**15**). This inhibitor was designed to trap the protosteryl cation through the allylic cation by introducing a vinyl group at C-20, which may then be covalently linked to a nearby nucleophilic residue in the active site (**Scheme 7**).[48] This study identified a so-called DCTAE motif that is strictly conserved among OSCs. The inhibitor was found to be attached to Asp residue of this motif, suggesting that the negative charge of Asp may stabilize the positive charge of the protosteryl cation intermediate. Later on, mutation of this Asp into the Asn of *S. cerevisiae* lanosterol synthase was found to abolish lanosterol synthase activity.[49] It was postulated that some acid residue such as Asp or Glu should be responsible for attacking an epoxide to initiate the cyclization reaction. In fact, mutation of all Asp and Glu residues that are conserved among five different lanosterol synthases from *C. albicans*, *S. cerevisiae*, *S. pombe*, rat, and human (six Asp residues and nine Glu residues in total) has shown that only the abovementioned Asp residue (Asp456 in *S. cerevisiae* ERG7 gene) was critical for lanosterol production.[49] Based on these results, Asp456 was proposed to be involved in the protonation of the epoxide rather than in stabilizing an intermediate carbocation.

Further information regarding the active site residues came from a random mutagenesis study. Mutant cycloartenol synthase (AtCAS1) clones that allowed yeast lanosterol synthase mutant (ergosterol auxotroph) to grow in the absence of exogenous ergosterol supply were selected. These clones were expected to produce lanosterol. One such clone was identified to have I481V mutation (AtCAS1 numbering).[50] This residue is located two residues upstream of the DCTAE motif. Careful analysis of the mutant showed the production of cycloartenol (**9**), lanosterol (**7**), and parkeol (**16**) to be in a 55:24:21 ratio. Parkeol (**16**) arose from C-9 carbocation **8** through deprotonation from C-11 (**Scheme 8**). Therefore, the residue at this position was proposed to control the final deprotonation step during C-8 or C-9 carbocation intermediate. In fact, all cycloartenol synthases identified so far possess Ile at this position. Conversely, a reverse mutation on lanosterol synthase, V454I mutation (*S. cerevisiae* ERG7 numbering), produced only lanosterol.[51] Therefore, Ile at this position in the context of AtCAS1 sequence is important for cycloartenol formation but not in an ERG background. Further substitution at this position by Ala or Gly resulted in monocyclic achilleol A (**17**) and camelliol C (**18**) produced through a monocyclic carbocation **1** (**Scheme 9**),[51,52] indicating that the residue at this position is also important for proper folding and cyclization beyond the monocyclic stage.

Numerous mutagenesis studies were further carried out, aided by the X-ray crystal structure of human lanosterol synthase, and have been are reviewed extensively.[53–55] These studies revealed several residues important for catalysis and product specificity, including Tyr410, His477, and Tyr532 of *A. thaliana* AtCAS1 and Trp232, His234, Thr384, Phe445, Tyr510, Phe699, and Tyr707 of *S. cerevisiae* ERG7. Most notably, just two

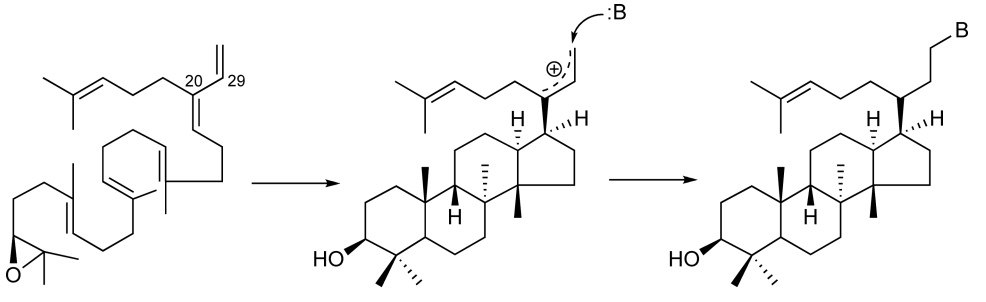

29-MOS (**15**)

Scheme 7

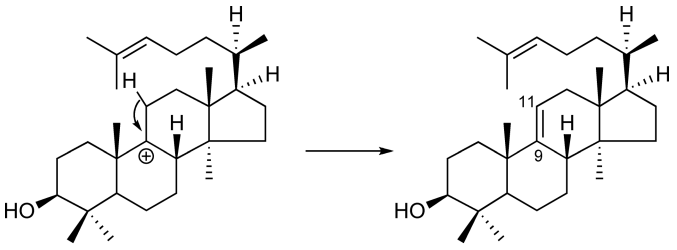

8 Parkeol (**16**)

Scheme 8

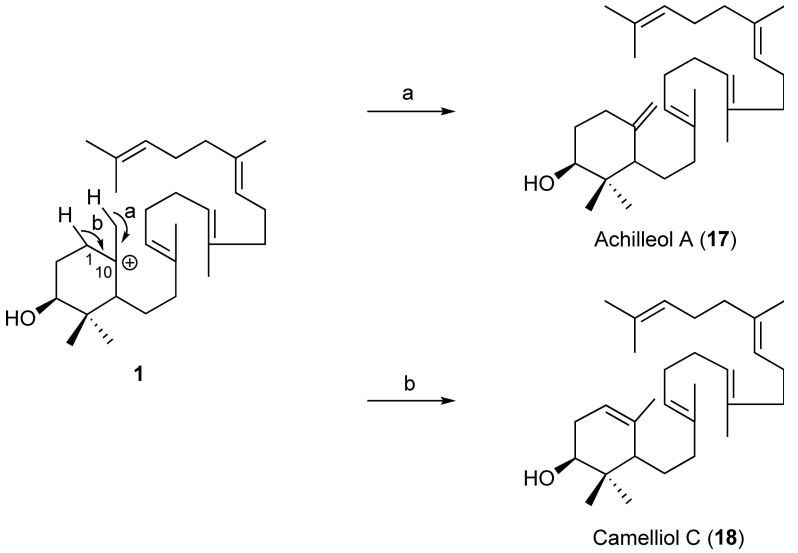

1

Scheme 9

mutations on AtCAS1, H477N/I481V, have converted cycloartenol synthase into nearly perfect lanosterol synthase (lanosterol:parkeol = 99:1).[56] According to the homology-modeled structure of AtCAS1, His477 is not located in an active site but in a second sphere located behind the active site residue Tyr410. It is remarkable how a small change in the amino acid residues of OSC can alter the cyclization reaction completely to produce other triterpenes.

1.18.3.4 Structure of Human Lanosterol Synthase

The X-ray crystal structure of human lanosterol synthase complexed with the product lanosterol was solved at 2.1 Å resolution (**Figure 5**).[24] The overall structure consists of two α/α barrel domains connected by several loops. The membrane-binding region is located in domain 2, which renders OSC as a monotopic membrane protein. The active site cavity is located in the center of the protein between the two domains and is connected to the surface through a narrow channel that protrudes into the membrane-binding region. This channel allows the substrate oxidosqualene to enter the hydrophobic active site from the membrane. Overall, the structure of OSC resembles that of SHC, despite showing only ~20% sequence identity. OSC has a smaller active site cavity than SHC, which may be important for controlling the substrate in the unstable B-ring *boat* conformation as opposed to *chair* in SHC, which requires minimal assistance from the enzyme.

The active site cavity is mainly hydrophobic, consisting of aromatic residues and a polar cap by Asp455 at the bottom of the cavity (**Figure 6**). Protonation of the substrate is mediated by this Asp residue, which is

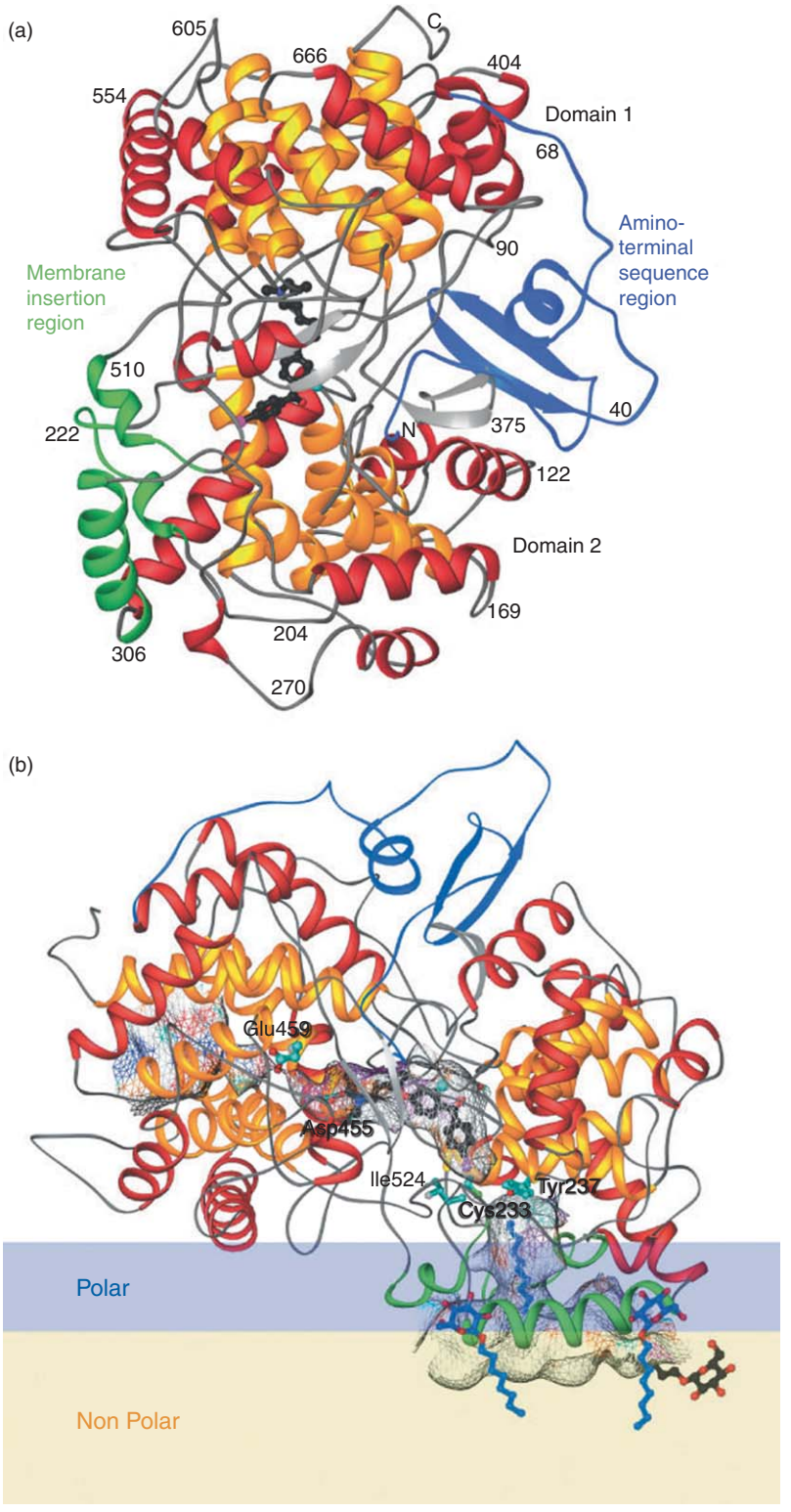

Figure 5 Crystal structure of human lanosterol synthase. (a) Ribbon diagram of the overall structure. The bound inhibitor molecule (Ro 48-8071) is shown in black and indicates the position of the active site. (b) The structure modeled within the membrane lipid bilayer. Detergent molecules found in the crystal are in blue.

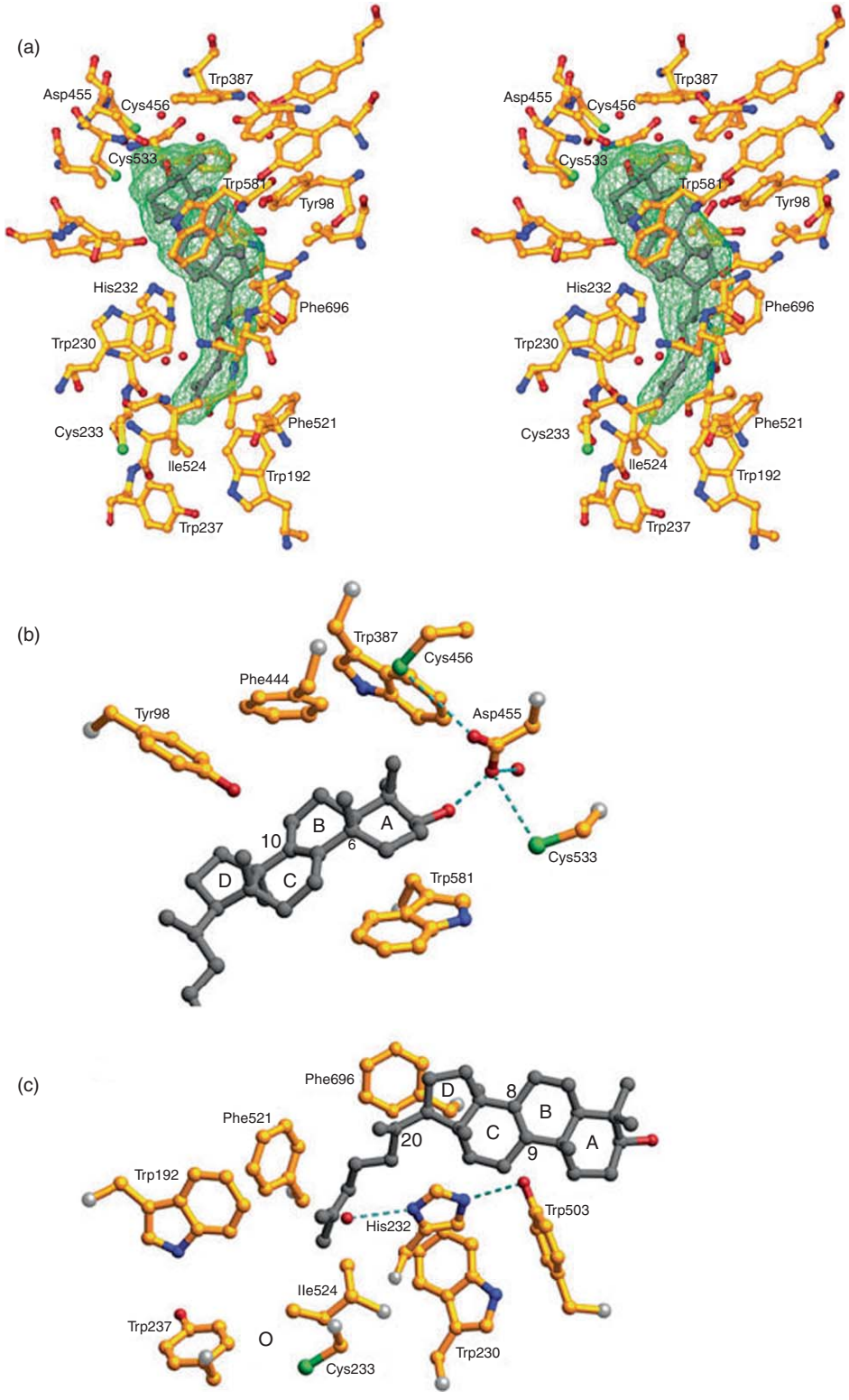

Figure 6 Stereoview of the active site cavity with bound lanosterol molecule. (a) Overall view of the active site. (b) The catalytic acid Asp455 with two Cys residues and aromatic residues that are postulated to be involved in the formation of A and B rings is shown. (c) Residues that are postulated to be involved in the formation of C and D rings are shown including His232 and Tyr503 hydrogen bond dyad, which plays a critical role in the final deprotonation process.

hydrogen bonded to nearby Cys residues that enhance the acidity of the Asp. The intermediate carbocations are stabilized through cation-π interaction by the aromatic residues that are suitably positioned to stabilize each different carbocationic intermediate. These hydrophobic residues also force the linear substrate to fold into a reactive conformation to allow cation-π cyclization to take place. The structure together with mutational studies has postulated the following picture for lanosterol formation.

The Asp455 residue assisted by two Cys residues (Cys456 and Cys533) is responsible for the initial proton attack on the epoxide to generate a carbocation. After the first ring formation, the monocyclic C-10 carbocation is stabilized by the Tyr503 residue. The second bicyclic C-8 carbocation is then stabilized by the Tyr704 residue, followed by the third 6-6-5 tricyclic C-14 carbocation by Tyr98 and His232 residues. The Tyr98 residue was also postulated to force the substrate into B-ring *boat* conformation. The fourth 6-6-6-5 protosteryl C-20 carbocation is then stabilized by His232 and Phe696 residues. The same Phe696 residue also stabilizes the first hydride rearranged C-17 carbocation as well. The Trp230 residue in the vicinity of His232 plays an important role during the hydride and methyl group shifts up to C-8 carbocation. Finally, both His232 and Tyr503 residues, which form a hydrogen bond dyad, play a critical role in the final deprotonation process. Mutations in these residues result in aberrant termination of the reaction to produce truncated products such as mono-, bi-, and tricyclic products as well as alternately deprotonated products.

1.18.4 Plant Triterpene Synthases

1.18.4.1 β-Amyrin and Lupeol Synthases

1.18.4.1.1 Mechanism

The majority of triterpenes found in nature are produced by higher plants. Over 100 different skeletal types of triterpenes are known.[7] These triterpenes can be classified according to the cyclization mechanism described below. In contrast to lanosterol and cycloartenol, most plant triterpenes are formed through oxidosqualene folded in a *chair–chair–chair* conformation in the active site of OSC. Similar to lanosterol and cycloartenol described above, cyclization initiated by a protonation of the epoxide generates carbocation intermediates **19–22** that result in tetracyclic dammarenyl cation **23** (**Scheme 10**). Comparing the structure of **23** with that of

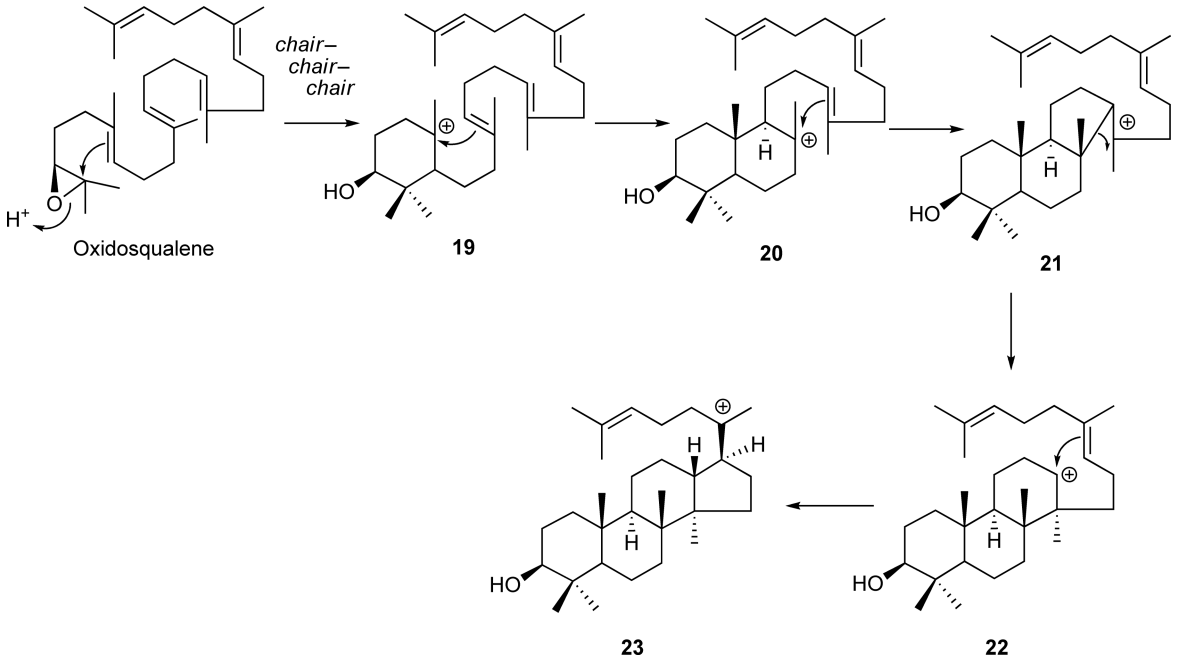

Scheme 10

the protosteryl cation (**5**) points to the differences in the stereochemistry around the C ring, which is due to the difference in B-ring conformation during cyclization (*chair* vs *boat*). Again, a ring expansion process is presumably involved during the third ring cyclization from the initially formed 6-6-5 fused system (**21**) to the 6-6-6 tricyclic intermediate (**22**) that eventually furnishes the 6-6-6-5 fused ring system of **23** (**Scheme 10**). A large number of triterpenes are derived from dammarenyl cation (**23**) such as dammarane, euphane, and tirucallane.

The most abundant triterpene found among higher plants by far is oleanane, which is derived from β-amyrin. β-Amyrin formation involves expansion of the D-ring of the dammarenyl cation from a five- to a six-membered ring, similar to C-ring expansion, which results in secondary C-18 baccharenyl cation (**24**) (**Scheme 11**). This is the basic carbon skeleton of the baccharane-type triterpenes. A subsequent fifth cyclization forms the five-membered E-ring carbocation intermediate known as a lupanyl cation (**25**). All lupane triterpenes originate from this intermediate, such as lupeol a (**26**), produced by deprotonation from one of the methyl groups. Another E-ring expansion would give the 6-6-6-6-6 cation **27** with a secondary C-19 carbocation, which is then followed by two hydride shifts from C-18 to C-19 and C-13 to C-18 to form an oleanyl cation (**28**). Final deprotonation of H-12α will produce β-amyrin (**29**). This transformation furnishes five ring systems and eight stereogenic centers in a single reaction.

1.18.4.1.2 Genes

The first triterpene synthase genes identified from plants were lupeol synthase from *A. thaliana* (AtLUP1)[57] and β-amyrin synthase from *P. ginseng* (PNY).[34] Both genes showed 30–40% synthase identities to animal and fungal lanosterol synthases, ~60% to cycloartenol synthase AtCAS1 and 70% to each other. They all contain QW motifs and the DCTAE motifs as well. Therefore, close evolutionary relationships between OSCs involved in triterpene biosynthesis and sterol biosynthesis have been revealed for the first time. The oleanane-type triterpenes that originate from β-amyrin are the most abundant triterpenes found in plants by far. β-Amyrin synthase genes have since been identified from a number of plants including *P. sativum*,[58] *G. glabra*,[59] *Avena strigosa*,[60] *B. platyphylla*,[39] *Medicago truncatula*,[61,62] *Euphorbia tirucalli*,[63] *L. japonicus*,[42] *Saponaria vaccaria*,[64] *Bruguiera gymnorrhiza*,[65] *Artemisia annua*,[66] *Aster sedifolius*,[67] and *A. thaliana*.[68] Except for *A. strigosa* bAS, all these genes share a substantial sequence identity (~80%) with each other and form a distinct clade in the phylogenetic tree. The monocot gene appears to diverge substantially from dicot genes.

AtLUP1 was initially described as lupeol synthase[57] but was later found to produce multiple products, including 3β,20-dihydroxylupane (**30**) (see Section 1.18.4.3).[69] A second type of lupeol synthase genes was cloned from *Olea europaea* (OEW) and *Taraxacum officinale* (TRW).[70] These lupeol synthases produced lupeol as the sole product. A sequence comparison between AtLUP1 showed ~60% amino acid sequence identity. It was later found that the second type of lupeol synthases was more widely found among such plants as including *B. platyphylla*,[39] *G. glabra*,[71] *R. communis*,[41] *L. japonicus*,[42] and *B. gymnorrhiza*.[65] Similar to β-amyrin synthases, these genes also form a distinct clade in the phylogenetic tree, demonstrating that OSCs with the same function exhibit a high sequence identity regardless of plant species.

A distinct stereochemical course of deprotonation from **25** during lupeol formation was identified between AtLUP1 and OEW/TRW.[72,73] Two terminal methyl groups of lupeol have a different biosynthetic origin, as one is derived from C-2 of mevalonate and the other from C-6 of mevalonate. These two methyl groups can be distinguished by feeding [1,2-$^{13}C_2$]acetate. According to the conventional mevalonate pathway, incorporating this doubly labeled acetate would form a triterpene in which carbon signals originating from C-2 of mevalonate appear as a singlet upon ^{13}C-NMR measurements, whereas those originating from C-6 appear with an accompanying doublet due to direct ^{13}C–^{13}C coupling resulting from retention of an intact acetate unit in the mevalonate molecule (**Scheme 12**). The feeding of [1,2-$^{13}C_2$]acetate into an AtLUP1-expressing yeast resulted in lupeol, where both C-29 and C-30 signals were accompanied by a doublet.[72] This indicated that deprotonation took place from both methyl groups. On the other hand, lupeol formed from OEW and TRW showed peaks in which C-29 appeared with an accompanying doublet with C-30 as a singlet.[73] Therefore, deprotonation took place only from the methyl group derived from C-6 of mevalonate, which corresponds to (*Z*)-methyl of oxidosqualene. These results indicated that OEW and TRW have strict control during the deprotonation step, whereas AtLUP1 appears to lack this control. Further study on the stereochemical course of a water addition to lupanyl cation (**25**) during 3β,20-dihydroxylupane (**30**) formation by AtLUP1 was carried out.[74]

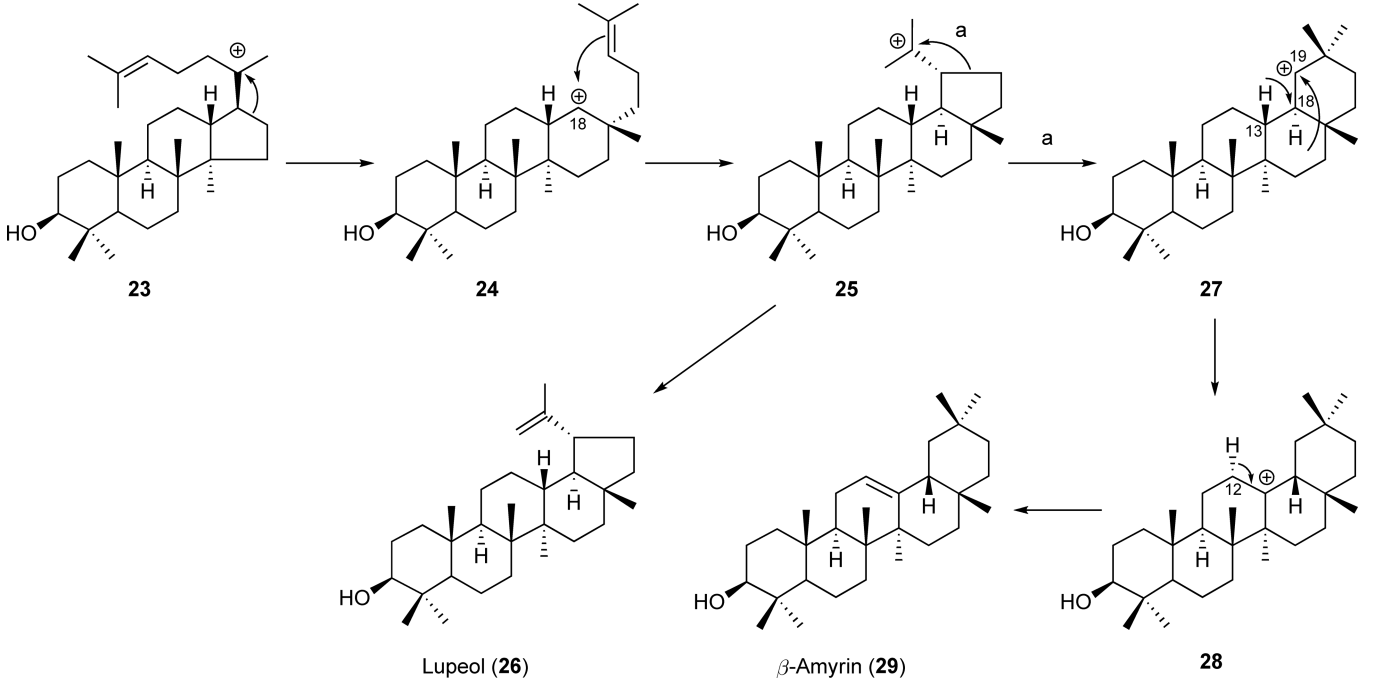

Scheme 11

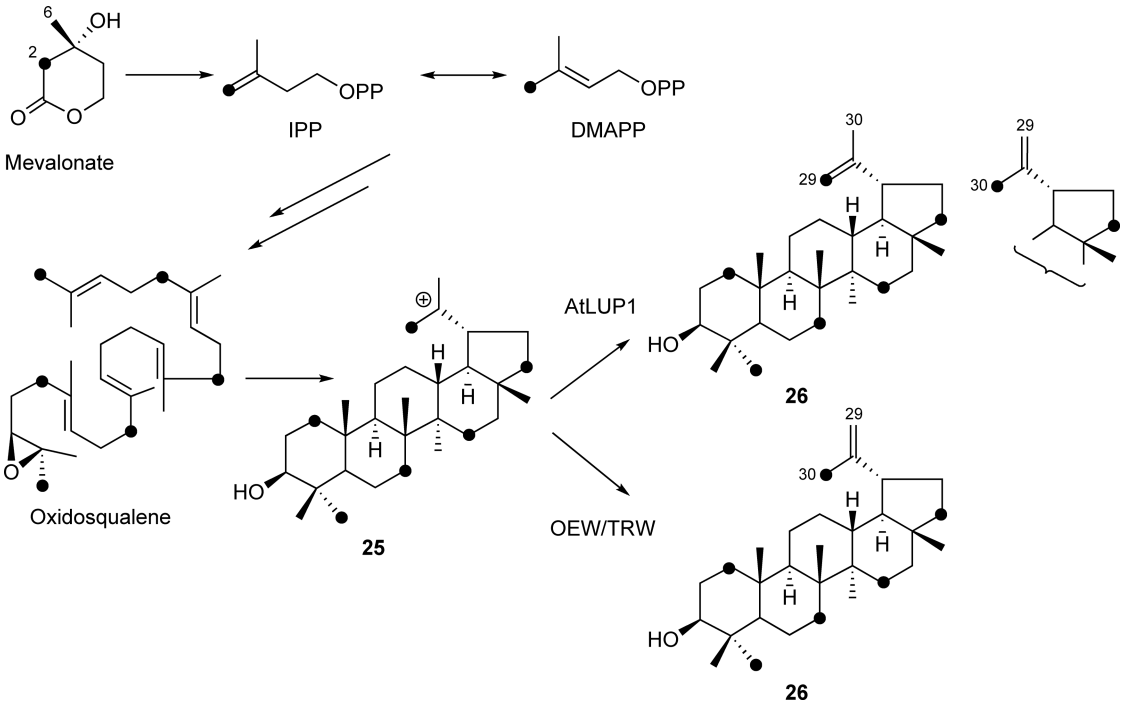

Scheme 12

The result showed stereospecific addition of a water molecule onto **25** discriminating the plane of the isopropyl cation moiety (**Scheme 13**). Taken together, AtLUP1 is a multifunctional OSC mainly producing lupeol (**26**) and 3,20-dihydroxylupane (**30**), whereas OEW and TRW are dedicated lupeol synthases.

1.18.4.1.3 Product specificity

By using lupeol synthase AtLUP1 and β-amyrin synthase PNY, amino acid residues that are responsible for controlling lupeol and β-amyrin formation during the cyclization reaction were investigated.[72,75] As mentioned above, formation of both triterpenes takes the same route up to the lupanyl cation stage **25**, where

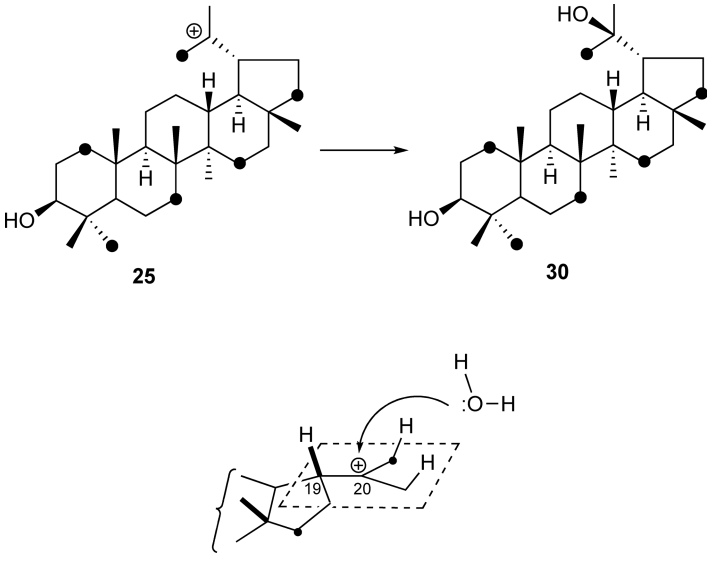

Scheme 13

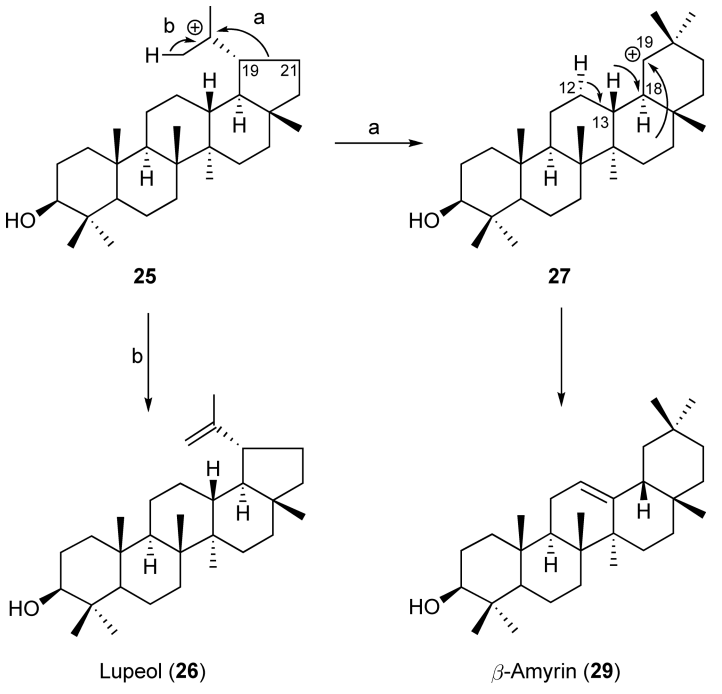

Scheme 14

deprotonation from a methyl group produces lupeol (**26**), whereas the C19–C21 bond migration to form a six-membered E ring, and two consecutive hydride migrations and a deprotonation of H-12α will produce β-amyrin (**29**) (**Scheme 14**). Any residues that control these two reactions should act at the lupanyl cation stage and divert the reaction path into each one.

Various chimeric proteins were made between AtLUP1 and PNY, and they have shown that the region important for β-amyrin formation resides on the 80 amino acid sequence region from Cys260 to Trp340 of PNY in the N-terminal half.[72] Sequence comparison of this region between several lupeol and β-amyrin synthases pointed to a sequence motif ^{258}MWCYC^{262} in PNY (MLCYC in OEW and ILCYS in AtLUP1). A Trp259 in this motif is strictly conserved among β-amyrin synthases, whereas it is conserved as Leu in all lupeol synthases. Mutation of the W259L of the PNY produced lupeol as a major product, whereas mutation of L256W of OEW produced β-amyrin as a major product (75%).[75] It is remarkable that OEW, which solely produces lupeol, already encompassed the potential ability to produce β-amyrin. This was evident from a single mutation that converted it to a nearly accurate β-amyrin synthase. Therefore, this Trp plays a critical role in controlling the reaction at the lupanyl cation stage to divert the reaction into β-amyrin pathway. The π electron of Trp may stabilize the secondary carbocation **27** to favor the E-ring expansion process, although a steric effect also cannot be ruled out. A Tyr261 of PNY in this motif is also highly conserved among lupeol and β-amyrin synthases, whereas it is His in all lanosterol and cycloartenol synthases. Therefore, involvement of this residue in regulating the fifth ring cyclization was suggested. Mutation of Y261H of PNY completely abolished β-amyrin production and produced novel tetracyclic triterpenes **31** and **32**.[75] These are dammarane types produced by a deprotonation from C-22 of dammarenyl cation **23** to form a mixture of E/Z isomer of $\Delta^{20(22)}$ (**Scheme 15**). The His residue, in place of Tyr, which would stabilize the secondary baccharenyl cation, might have served as a base to abstract proton from C-22 at the dammarenyl cation stage. These studies demonstrated that product specificity is controlled by relatively few residues of OSC.

1.18.4.2 Multifunctional Triterpene Synthase

Besides lupeol and β-amyrin synthases, the cloning of OSCs from higher plants has revealed the existence of multifunctional triterpene synthases that produce several products simultaneously. These results argue

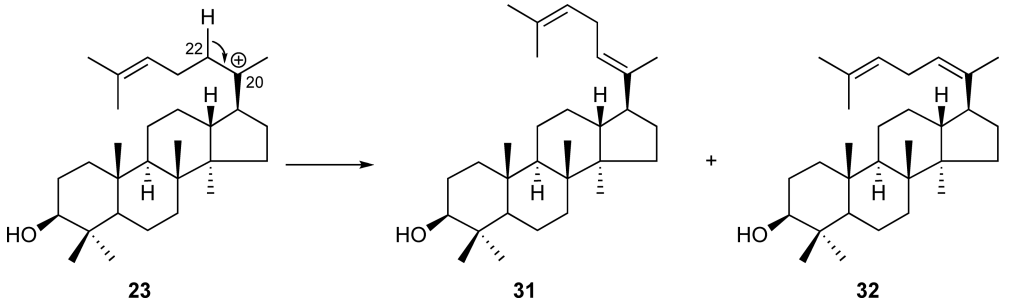

Scheme 15

against the existence of product-specific OSCs for each of the 100 different triterpene skeletons found in nature so far. Therefore, the number of OSC genes is probably much smaller than the actual number of triterpene skeletons found.

The triterpene synthase that produces α-amyrin, the basic carbon skeleton of ursane-type triterpenes, which are the second major types found in higher plants, was identified from *P. sativum* (PSM).[58] However, it was found to be a multifunctional OSC producing α-amyrin (**36**) (50%) and β-amyrin (**29**) (34%) in nearly equal amounts, together with several minor triterpenes including δ-amyrin (**40**) (8%), Ψ-taraxasterol (**41**) (5.3%), butyrospermol (**37**) (3.4%), lupeol (**26**) (1.3%), germanicol (**39**) (<1%), and taraxasterol (**42**) (<1%). α-amyrin (**36**) formation involves methyl group migration from C-20 during carbocation **27** to result in a taraxasteryl cation (**33**), from which three consecutive hydride shifts from C-19 to C-20, C-18 to C-19, and C-13 to C-18 take place to result in a ursanyl cation (**35**). A final deprotonation of H-12β will produce α-amyrin (**36**) (**Scheme 16**). On the other hand, butyrospermol (**37**) is formed from a dammarenyl cation (**23**) through two hydride and two methyl group shifts and a final deprotonation from C-7 (**Scheme 17**), whereas germanicol (**39**) and δ-amyrin (**40**) are formed from a deprotonation from cation **27** and germanicyl cation (**38**), respectively (**Scheme 18**). Both Ψ-taraxasterol (**41**) and taraxasterol (**42**) arose from a taraxasteryl cation (**33**) by a

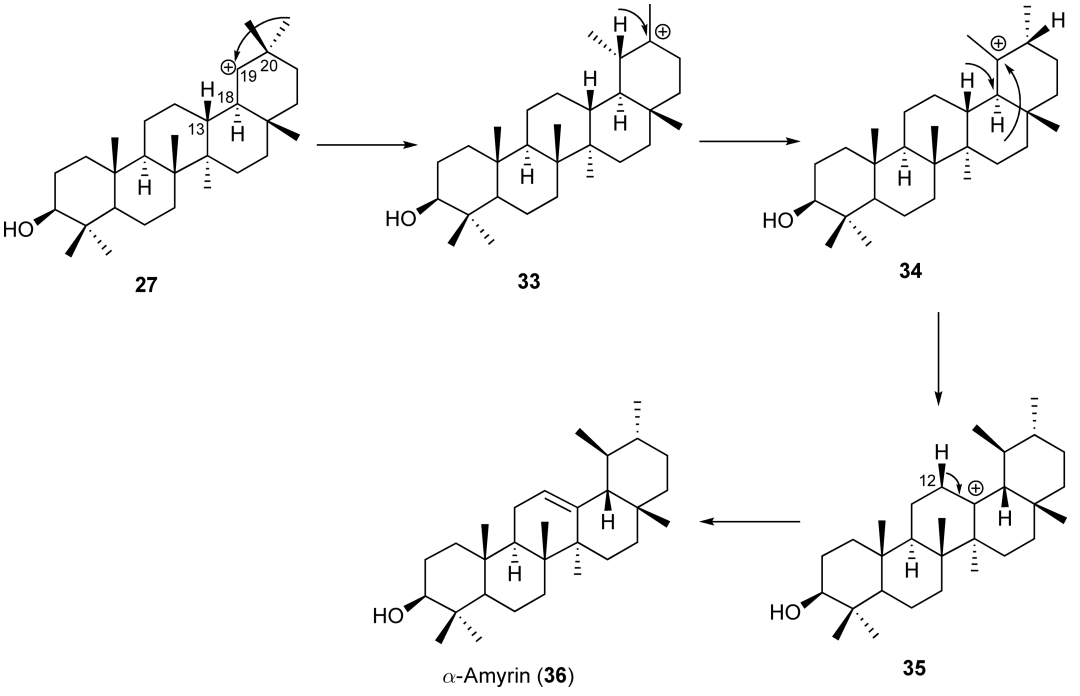

Scheme 16

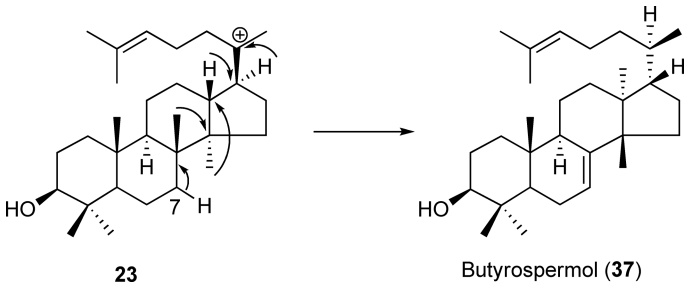

Scheme 17

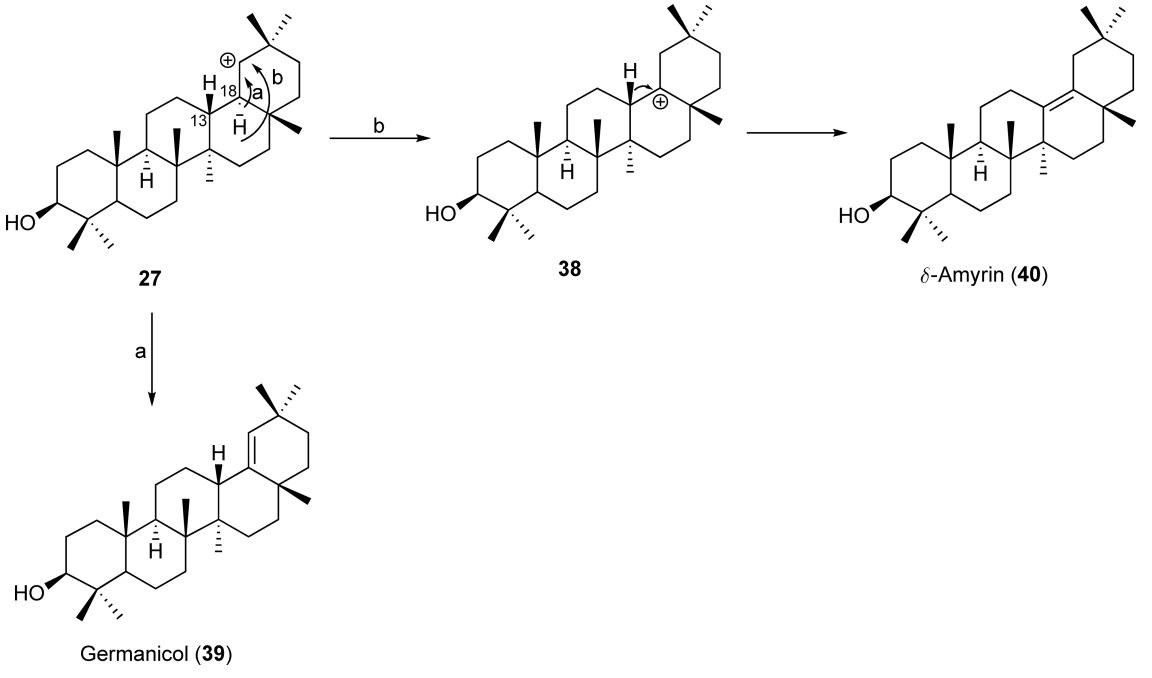

Scheme 18

deprotonation from C-21 and from methyl group C-30, respectively (**Scheme 19**). PSM and AtLUP1 are one of the first multifunctional triterpene synthases to be identified. A product-specific β-amyrin synthase PSY was also found from *P. sativum* and exhibited 78% sequence identity with PSM.[58] A remarkable sequence identity and a difference in the product outcome pose an intriguing question as to how plants have evolved such OSCs to produce a myriad of triterpene products. Formation of α- and β-amyrin, two of the most popular triterpenes found in higher plants, shares the common carbocationic intermediate **27**. A methyl group shift from C-20 (C-30 methyl group) would eventually lead to α-amyrin, whereas a hydride shift from C-18 would give β-amyrin (**Scheme 20**). Therefore, in PSM, competition between methyl and hydride migration takes place to produce both triterpenes in nearly the same amounts. Formation of other minor products indicates that the reaction control is not strict in PSM and that these products arose from termination of a reaction at several intermediate carbocationic species. The existence of such multifunctional enzymes is characteristic of terpene cyclases in general and implies that nature has allowed to evolve such nonspecific cyclases that lost control over the cyclization reaction. This may have an advantage in plants that utilize a myriad of terpenoid products for defense purposes. Until now, none of the α-amyrin-specific OSCs has been cloned. This may imply that α-amyrin is always produced together with β-amyrin by multifunctional OSCs. Several multifunctional OSC genes have been cloned from *C. speciosus*,[38] *L. japonicus*,[42,62] *K. candel*,[76] *O. europaea*,[77] and *R. stylosa*.[65]

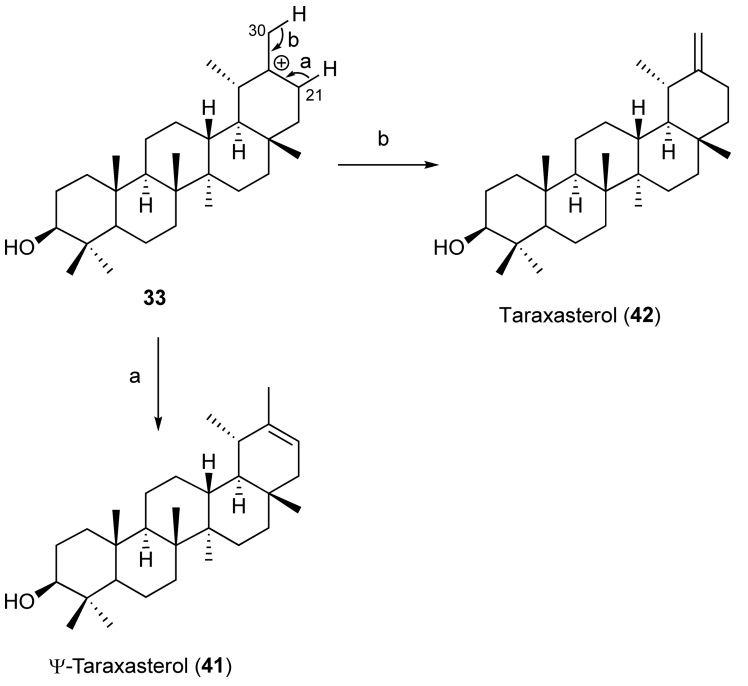

Scheme 19

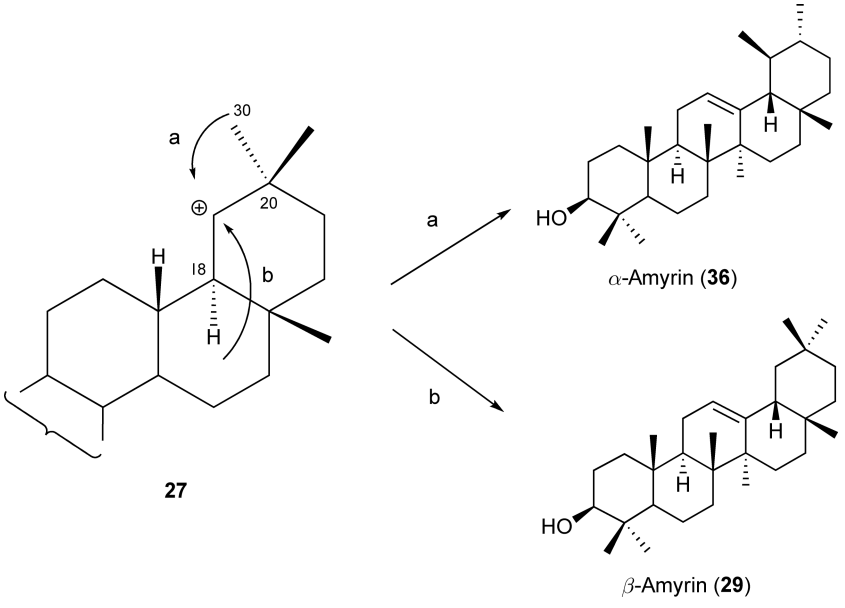

Scheme 20

1.18.4.3 *Arabidopsis* Triterpene Synthases

The whole genome sequencing of *A. thaliana* has revealed the existence of 13 OSC genes in the genome. Serving as a model plant, it was of general interest to identify the function of these OSCs. Most of these genes have now been functionally characterized and have uncovered a remarkable catalytic potential of OSC that had not been seen before. These *A. thaliana* OSC genes form distinct branches on the phylogenetic tree, which indicates that these genes evolved independently in this plant lineage.

AtCAS1 (At2g07050) is the first identified cycloartenol synthase from any plants that are responsible for sterol biosynthesis.[32] The gene was found to be essential for sterol biosynthesis in *A. thaliana*. A knockout of the gene caused growth arrest of shoot and root meristems and abnormal growth of leaves as well as albino phenotype in inflorescence shoots resulting from defect in plastid biogenesis.[78]

AtLUP1 (At1g78970) is a multifunctional triterpene synthase that mainly produces lupeol (**26**) (39%) and 3β,20-dihydroxylupane (**30**) (39%), together with minor amounts of β-amyrin (**29**) (8%), germanicol (**39**) (7%), Ψ-taraxasterol (**41**) (4%), and taraxasterol (**42**) (3%).[69] Therefore, AtLUP1 mainly forms a lupanyl cation (**25**); however, minor amounts of cation **27** and taraxasteryl cation (**33**) are also formed.

At1g78960 (LUP2) is a multifunctional triterpene synthase that produces nine triterpenes in total,[79] including lupeol (**26**), β-amyrin (**29**), α-amyrin (**36**), taraxasterol (**42**), Ψ-taraxasterol (**41**), butyrospermol (**37**), tirucalla-7,24-diene-3β-ol (**43**), multiflorenol (**44**), and bauerenol (**45**). Although production of taraxasterol and β-amyrin was slightly higher than the other triterpenes, the product ratio of all nine triterpenes was more or less the same. Tetracyclic tirucalla-7,24-diene-3β-ol (**43**) is derived from the dammarenyl cation (**23**) similar to butyrospermol but differs in the stereochemistry at C-20 (**Scheme 21**). Perhaps, the side-chain orientation is different between the two prior to H-17α hydride migration. On the other hand, multiflorenol (**44**) and bauerenol (**45**) are rather rare triterpenes found in plants, and they are derived from oleanyl (**28**) and ursanyl cation (**35**) intermediates through hydride and methyl migration. Again, the reactions are terminated by a deprotonation from C-7 (**Scheme 22**). Therefore, this OSC significantly lacks control over carbocationic intermediates and allows the reaction to terminate at various intermediate stages, for example, dammarenyl cation (**23**), lupanyl cation (**25**), taraxasteryl cation (**33**), oleanyl cation (**28**), and ursanyl cation (**35**). Four out of nine products arose from a deprotonation from C-7, which may suggest that this OSC has to have a strong basic residue around this position. The multiplicity of triterpenes produced by this OSC is unprecedented. Because this OSC exhibited a 79.4% sequence identity with AtLUP1, a region responsible for such a product multiplicity was sought.[79] Several chimeric proteins were made, and it was found that a C-terminal half and a part of an N-terminus were important for the observed multiplicity in At1g78960.

At1g78955 (CAMS1, LUP3) produces monocyclic camelliol C (**18**) (98%) as a major product, together with minor amounts of achilleol A (**17**) (2%) and β-amyrin (**29**) (0.2%).[80] These monocyclic products were derived from cation **1** through a deprotonation from C-1 for camelliol C (**18**) and depronation from a C-10 methyl group (C-25) for achilleol A (**17**) (**Scheme 9**). This is the first triterpene synthase that produces monocyclic triterpene as a major product. Such monocyclic products were produced in several lanosterol and cycloartenol synthase mutants mentioned above whose normal cyclization was aberrantly disrupted at a monocyclic stage. Interestingly, sequence comparison has indicated that this OSC harbors Ala at a position two residues upstream of the DCTAE motif where most plant triterpene synthases and lanosterol synthases contain Val, and whereas cycloartenol synthases contain Ile. This Ile was shown to be important for cycloartenol (**9**) formation as described above. Because overall sequence identity shows CAMS1 to be more closely related to LUP1 and LUP2 (71%), which produce polycyclic triterpenes, this monocyclic-producing OSC may have evolved from a polycyclic-producing OSC one through loss-of-function mutation such as Val to Ala at the critical residue that controls the reaction at a monocyclic intermediate stage. Production of minor amounts of β-amyrin (**29**) was suggested to be an evolutionary remnant of this event.

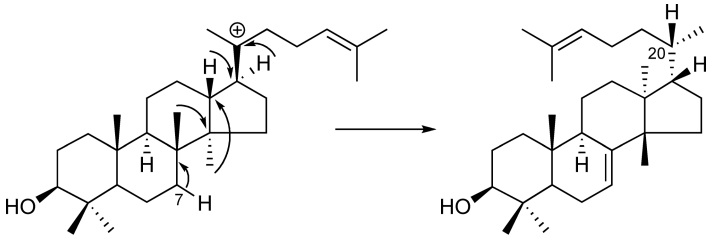

23 Tirucalla-7,24-diene-3β-ol (**43**)

Scheme 21

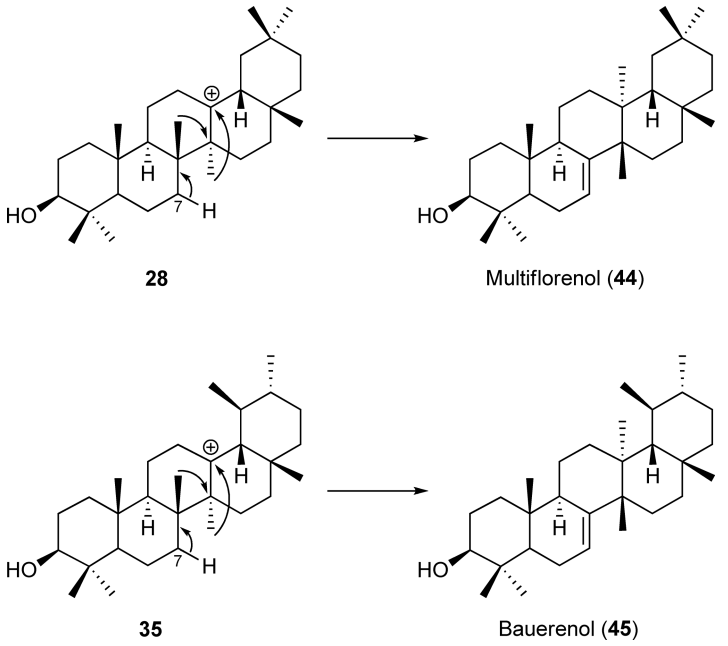

Scheme 22

At1g78950 (AtBAS) produces almost exclusively β-amyrin (**29**) together with trace amounts of some triterpenes including butyrospermol (**37**).[68] Therefore, AtBAS was designated as the β-amyrin synthase of *A. thaliana*. LUP1, LUP2, CAMS1, and AtBAS are all located in tandem on chromosome 1 and may have evolved through a tandem duplication, as they all exhibit a high sequence identity to each other.

Notably, At1g66960 (LUP5) produces three products, of which one has been identified as tirucalla-7,21-dien-3β-ol (**43**).[81]

At5g48010 (THA1, PEN4) produces a tricyclic malabaricane-type triterpene named thalianol (3*S*,13*S*,14*R*)-malabarica-8,17,21-trien-3-ol (**46**) as the sole product.[82] Thalianol (**46**) is derived from 6-6-5 fused tricyclic carbocation **21**, which undergoes a hydride shift from C-13 to C-14 and a methyl shift from C-8 to C-13, followed by a deprotonation from C-9 (**Scheme 23**). Thalianol is a novel triterpene and such a rearranged malabaricane is very rare in plants. A C-3 analog has been identified from ferns.

At4g15340 produces a similar tricyclic malabaricane-type triterpene with two hydroxyl groups named arabidiol (3*S*,13*R*)-malabarica-17,21-dien-3,14-diol (**47**).[83] Arabidiol (**47**) is derived from the same tricyclic carbocation **21** by the addition of water without any rearrangements (**Scheme 24**). The stereochemistry of the tertiary alcohol was deduced to be 14*R* as shown in **Scheme 24**, which suggests that a water attack on a carbocation takes place from the sterically less hindered side of carbocation **21**.[84] This OSC also produces 14-epithalianol (**48**) as a minor product.[84]

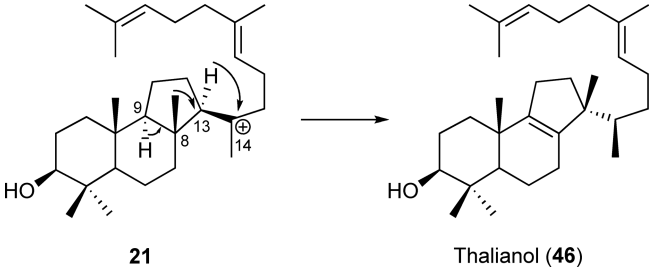

Scheme 23

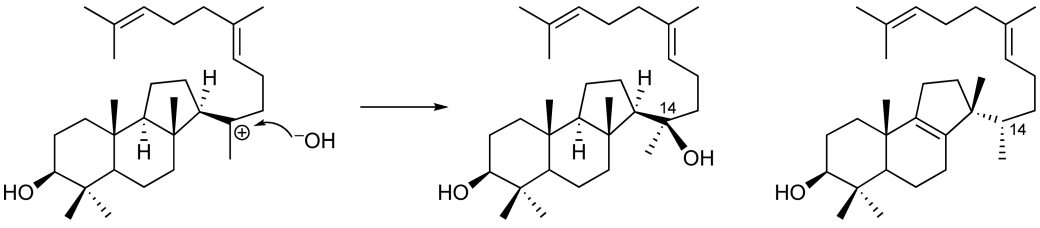

Scheme 24

Surprisingly, At3g45130 (LSS1, LAS1) produces lanosterol (**7**) as the sole product and is the first lanosterol synthase to be identified from the plant kingdom.[29,30] It had been long believed that plants produce cycloartenol (**9**) as a cyclization product of oxidosqualene and that cycloartenol serves as a precursor for all plant sterols, although some plants were found to contain lanosterol. This lanosterol was believed to be derived from cycloartenol through rearrangement of the cyclopropane ring to form a Δ^8 structure. With the discovery of lanosterol synthase in plants, the physiological role of lanosterol in plants is highly intriguing and may have a role in supporting the biosynthesis of some phytosterols. Recent studies, however, indicated a very minor contribution of LAS1 toward sterol biosynthesis in *A. thaliana*. The majority of are still produced by the cycloartenol synthase, AtCAS1.[85] Lanosterol synthase genes have also been identified from *P. ginseng*[30] and *L. japonicus*.[31] These plant lanosterol synthases share a high sequence identity with cycloartenol synthases from plants (~65%) than with fungal (~35%) or mammalian (~40%) lanosterol synthases, indicating a close evolutionary relationship with plant cycloartenol synthases. However, all critical residues that dictate cycloartenol or lanosterol formation were found the lanosterol type. For example, both Asn and Val residues were found in the place that corresponds to His477 and Ile481, respectively, of AtCAS1. As mentioned above, mutations in these two residues of AtCAS1 (H477N/I481V) have converted cycloartenol synthase into a nearly perfect lanosterol synthase.[56]

At5g42600 (MRN1, PEN5) produces *seco* triterpene aldehyde **50** named marneral,[86] the basic carbon skeleton of iridals, and arose through a ring-A cleavage of a bicyclic skeleton. The cyclization mechanism can be rationalized as follows (**Scheme 25**). The formation of AB rings involves oxidosqualene folded in *chair–boat* conformation. The B-ring boat conformation is rather unusual among plant triterpenes. The intermediate carbocation **2** then undergoes hydride shift from C-9 to C-8 followed by a methyl group shift from C-10 to C-9 and a hydride shift from C-5 to C-10 to result in carbocation **49**. This then undergoes Grob fragmentation through hyperconjugation of C3–C4 σ bond with C-5 carbocation to give *seco* aldehyde **50**. It is somewhat remarkable that this OSC allows only the C-5 carbocation to undergo Grob fragmentation, despite other pathways such as a deprotonation from C-6 to give a Δ^5 structure or a 4β-methyl migration from C-4 followed by 3α-hydride shift to give a 3-keto structure. It has been proposed that it is the B-ring conformation and the flexibility of a presumed Asp residue that abstracts a proton from a C-3 hydroxyl group that are important factors for this Grob fragmentation selectivity. This was the first observation of OSC catalyzing a preformed ring cleavage to produce a *seco* triterpene. Iridals have been only found from Iridaceae plants. In addition to **50**, this OSC also produces minor amounts of achilleol A (**17**) and camelliol C (**18**).

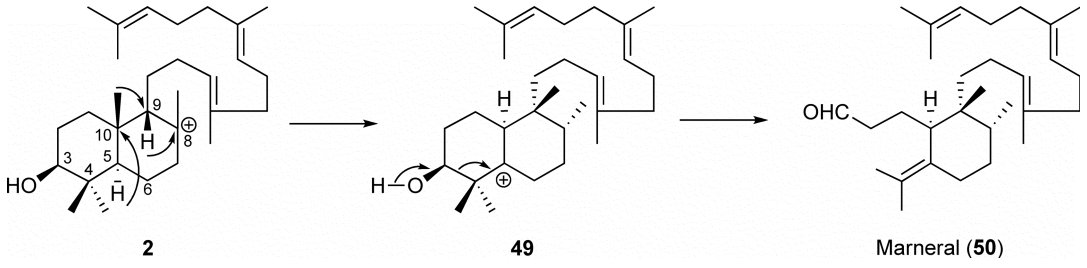

Scheme 25

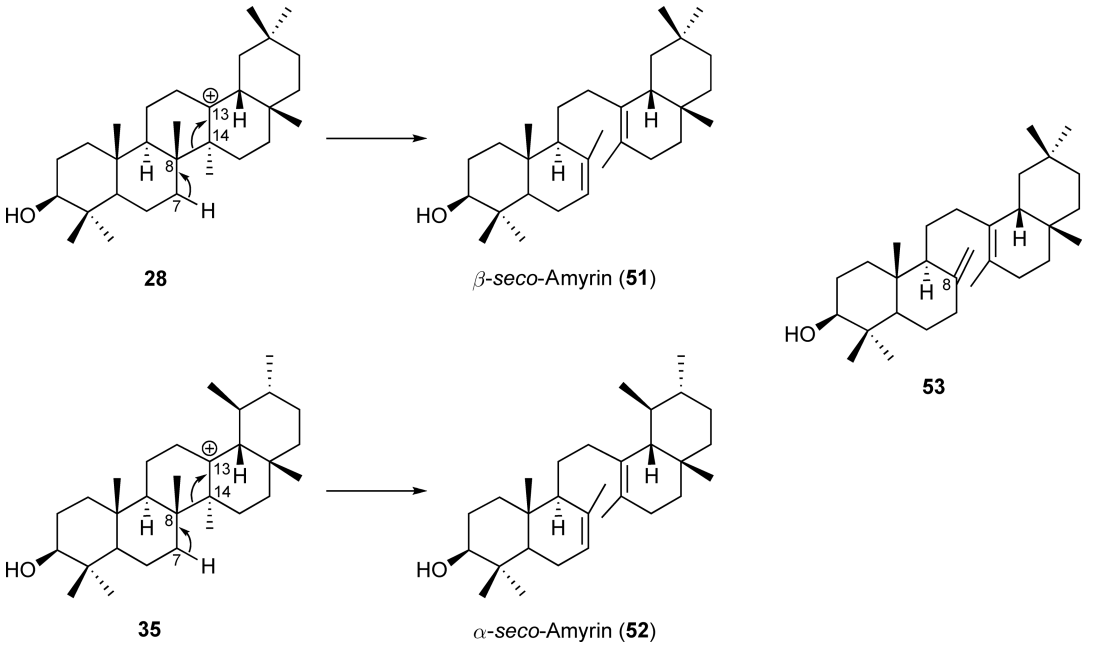

Scheme 26

At1g78500 (PEN6) produces a mixture of triterpenes, but most notably produces *seco* triterpenes **51** and **52**. These are oleanane and ursane types of C-ring *seco* triterpenes.[87] These *seco* triterpenes arose from oleanyl (**28**) and ursanyl (**35**) cations through Grob fragmentation, which results in C-ring cleavage between C-8 and C-14 to form a C13–C14 double bond followed by a deprotonation from C-7 to give a C7–C8 double bond (**Scheme 26**). These are other examples of OSC catalyzing the formation of *seco* triterpenes. Compounds **51** and **52** are *β-seco*-amyrin and *α-seco*-amyrin, respectively. Only the *β-seco*-amyrin-type triterpene (**53**) has been isolated from plants, *Stevia viscida* and *S. eupatoria*, with an *exo*-methylene at C-8. Besides **51** and **52**, this OSC produces lupeol (**26**), α-amyrin (**36**), and bauerenol (**45**) as well.[81]

Finding these *seco* triterpene-producing OSCs has led to the proposal that other natural *seco* triterpenes may also be products of OSCs. Such products include graminol A (**54**),[88] helianol (**55**),[89] sasanquol (**56**),[90] camelliol A (**57**),[91] and camelliol B (**58**)[91] (**Figure 7**). Notably, camelliol B can be regarded as an A/B/C-ring *seco* triterpene.

At4g15370 (BARS1) produces almost exclusively baruol (**61**) (90%) and 22 minor triterpenes (0.02–3% each).[92] Baruol (**61**) is a baccharane-type triterpene derived from baccharenyl cation **24** through extensive hydride and methyl shifts (six in total) to generate C-5 carbocation **60**, which is followed by a deprotonation from C-6 (**Scheme 27**). The minor products include lemmaphylladienol (**62**) and columbiol (**63**), which arose from the intermediate carbocation **59** through a deprotonation from C-7 and C-9, respectively, and sasanqual (**64**). Sasanqual is another example of an A-ring *seco* triterpene formed from OSC. The ability of this OSC to generate such a multitude of products is remarkable.

1.18.4.4 Other Triterpene Synthases

1.18.4.4.1 Isomultiflorenol synthase

Isomultiflorenol synthase (IMS) gene was cloned from *Luffa cylindrica* cell suspension culture,[93] which is known to produce bryonolic acid, a C-29 oxidized form of isomultiflorenol. Isomultiflorenol (**65**) arose from oleanyl cation (**28**) through two methyl group shifts to generate the C-8 carbocation from which a deprotonation from C-9 takes place to give Δ^8 (**Scheme 28**). IMS exhibited a 65% sequence identity with *β*-amyrin synthase (PNY) and a 57% sequence identity with lupeol synthase (OEW). A rather high sequence identity with *β*-amyrin synthase is reasonable considering that **65** is formed from the same intermediate oleanyl cation (**28**).

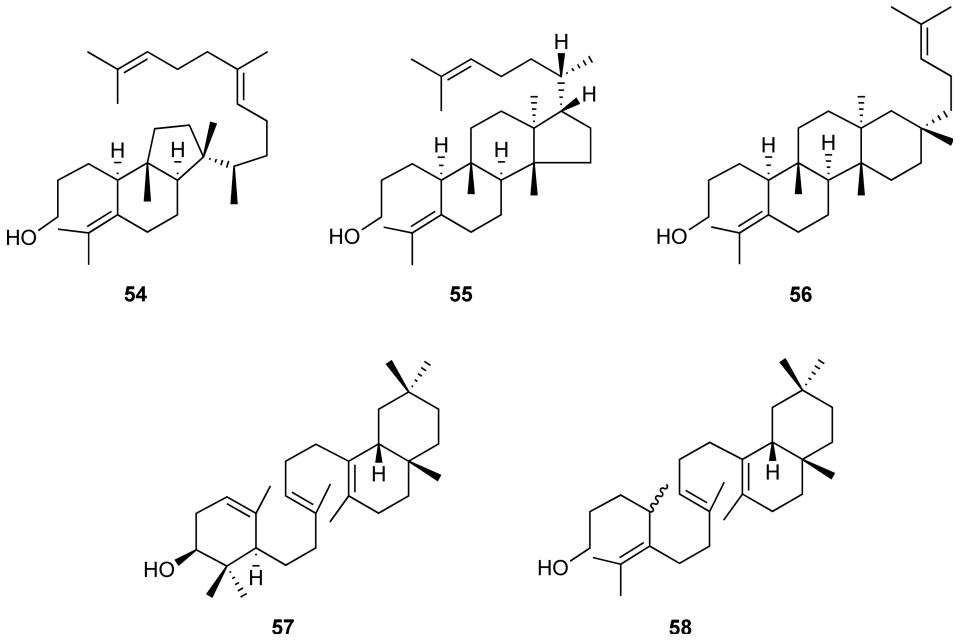

Figure 7 Structures of natural *seco* triterpenes found in plants.

1.18.4.4.2 Dammarenediol synthase

(20*S*)-Dammarenediol (**66**) is the basic skeleton of triterpene saponins from *P. ginseng*, known as ginsenosides, the most popular and widely used Chinese traditional medicine. It is derived from tetracyclic dammarenyl cation (**23**) by a stereospecific water addition onto C-20 (**Scheme 29**). The stereochemistry at C-20 of the enzymatically formed product was rigorously proven to be 20*S*.[94] All the naturally occurring ginsenosides have a 20*S* configuration; however, when *P. ginseng* is treated with steam water to produce red ginseng, some ginsenosides with a 20*R* configuration are produced. This epimerization at C-20 through dehydration and rehydration is assisted by a 12β-hydroxyl group.[95] Dammarenediol synthase (PNA) was cloned from *P. ginseng* hairy root culture[96] and exhibited ~57% sequence identity with β-amyrin synthase (PNY) and lupeol synthase (OEW). This is one of the rare cases in OSC that the reaction is terminated by adding water to a carbocationic center. Other OSCs known to produce such hydroxylated products are AtLUP1, which gives 3β,20-dihydroxylupane (**30**), and At4g15340, which gives arabidiol (**47**).

1.18.4.4.3 Cucurbitadienol synthase

Cucurbitane types are exceptional plant triterpenes that arose from protosteryl cation (**5**), which is formed by oxidosqualene folded in a *chair–boat–chair* conformation as in lanosterol (**7**) and cycloartenol (**9**). Cucurbitadienol (**68**) biosynthesis follows the same pathway with cycloartenol (**9**) up to C-9 carbocation intermediate **8**, where a further methyl shift from C-10 to C-9 and a hydride shift from C-5 to C-10 give C-5 carbocation **67**. A deprotonation from C-6 will furnish Δ^5 (**Scheme 30**). Cucurbitacins are highly oxygenated triterpenes characteristic of Cucurbitaceae plants and are often associated with a bitter taste such as in cucumber or *Momordica charantia*. Cucurbitadienol synthase (CPQ) was cloned from pumpkin *Cucurbita pepo*[40], and the amino acid sequence of CPQ showed a high sequence identity (~68%) with cycloartenol synthases, which is reasonable considering the resemblance of the cyclization mechanism. It contains Ile at the position two residues upstream of the DCTAE motif (corresponds to Ile481 of AtCAS1). CPQ and cycloartenol synthases are the only OSCs that harbor Ile at this position and presumably this Ile plays an important role in the generation of C-9 carbocation and beyond.

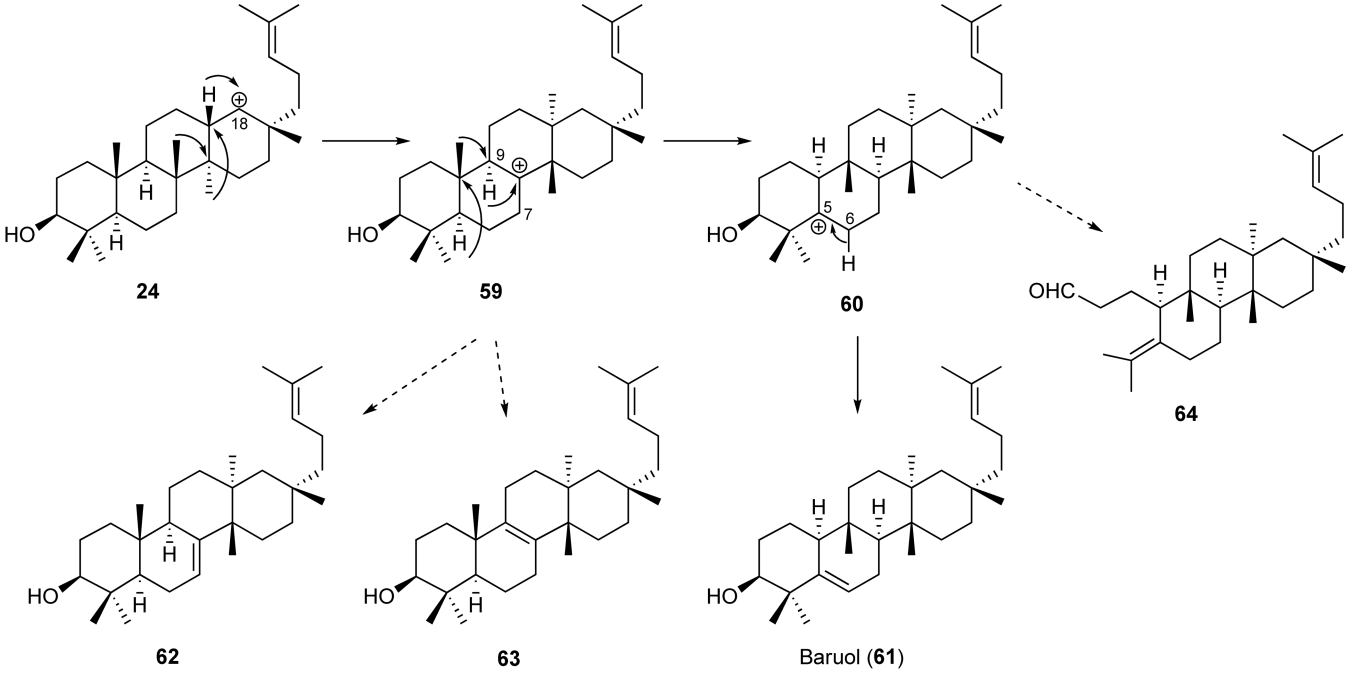

Scheme 27

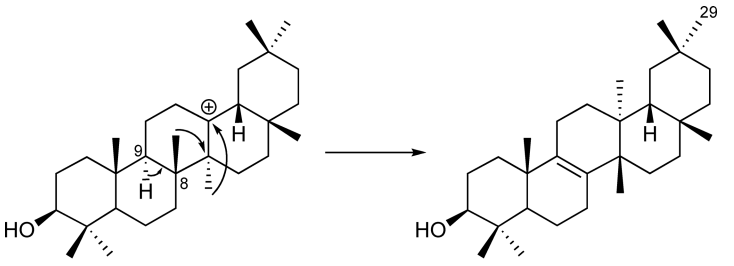

28 Isomultiflorenol (**65**)

Scheme 28

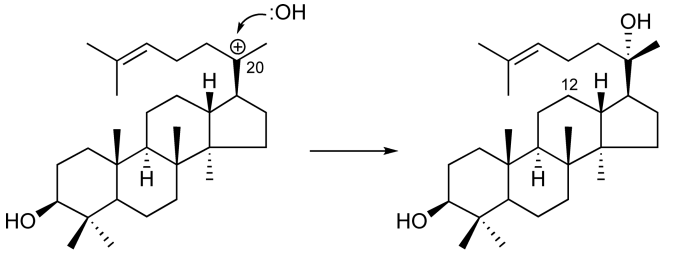

23 (20*S*)-Dammarenediol (**66**)

Scheme 29

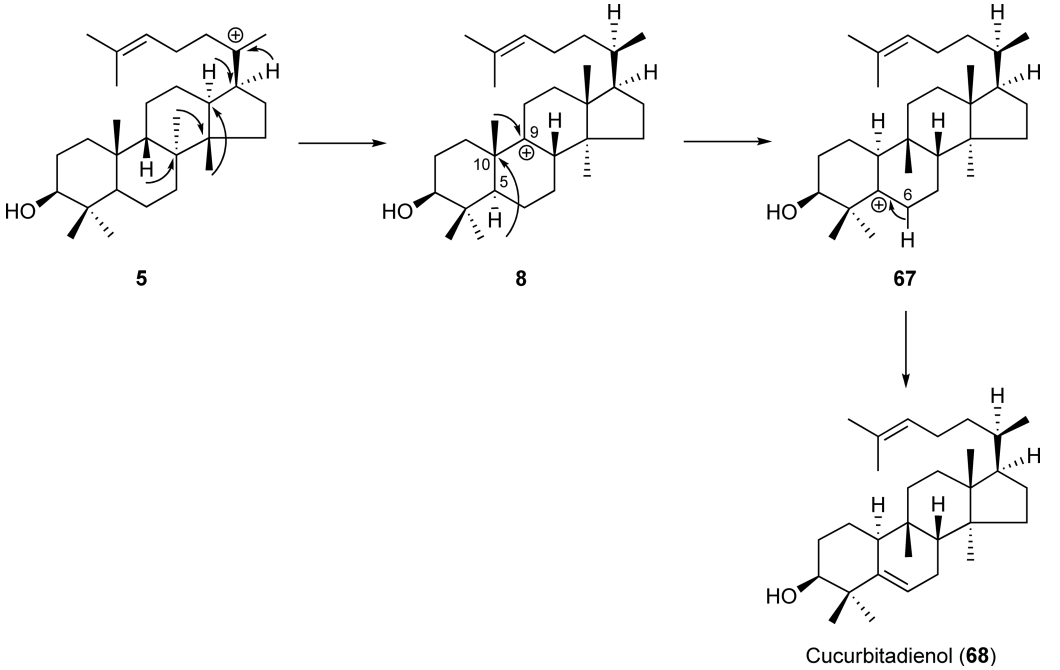

5 **8** **67**

Cucurbitadienol (**68**)

Scheme 30

1.18.4.4.4 Baccharis oxide synthase

The baccharis oxide (**70**) belongs to a baccharane-type triterpene that has an unusual C3–C10 oxide bridge over the A ring. The baccharis oxide is derived from baccharenyl cation (**24**) by a sequence of methyl and hydride shifts to give C-10 carbocation **69** to which the OH group at C-3 attacks to terminate the reaction (**Scheme 31**). Such an ether bridge in triterpene is found only in dendropanoxide (**71**), which is derived from an oleanyl cation (**28**).[97] The baccharis oxide has been isolated from Asteraceae plants. The baccharis oxide synthase (BOS) gene was cloned from *S. rebaudiana* and was also found to produce minor amounts of achilleol A (**17**), camelliol C (**18**), baruol (**61**), sasanquol (**56**), euphol (**72**), butyrospermol (**37**), and β-amyrin (**29**).[98] Production of **70** was 75% of the total products. Euphol (**72**) belongs to the euphane type, the same as butyrospermol (**37**), and arose from a dammarenyl cation (**23**) through two hydride and two methyl group shifts and a final deprotonation from C-9 (**Scheme 32**). This gene showed an ~70% sequence identity with β-amyrin synthases and an ~57% identity with lupeol synthases. BOS is characterized in having a Thr residue at the position two residues upstream of the DCTAE motif, which is normally Val or Ile (or Ala in *A. thaliana* CAMS1). Whether or not this Thr plays a role in oxide bridge formation remains to be studied. Evidently, this OSC forces the intermediate to adopt an A-ring *boat* conformation in order to allow an attack of the C-3 OH group onto the C-10 carbocation.

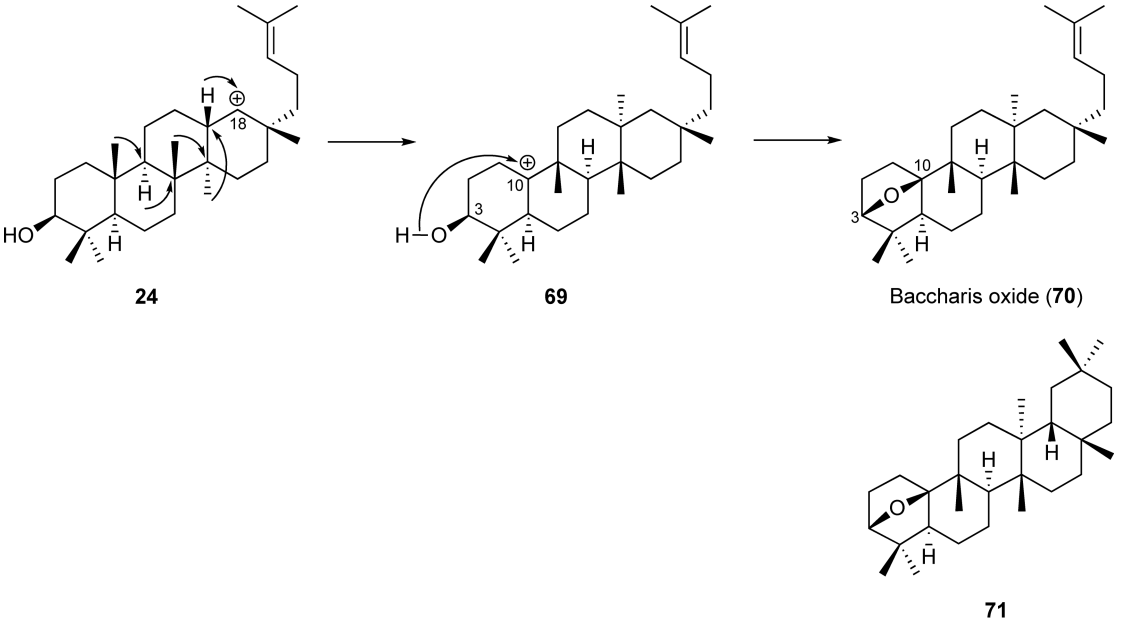

Scheme 31

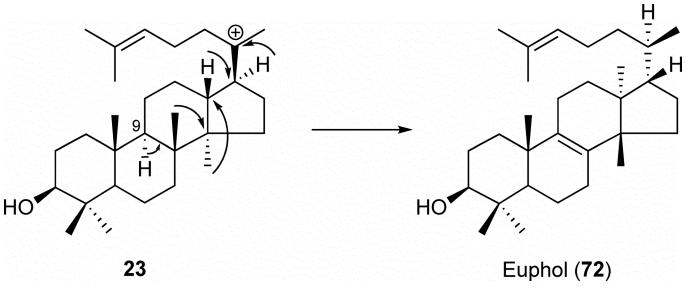

Scheme 32

1.18.4.4.5 Protostadienol synthase

A fungal OSC that produces protosta-17(20)*Z*,24-dien-3β-ol (**73**), which is the basic carbon skeleton of fusidanes, was cloned from the fungus *Aspergillus fumigatus*.[99] Compound **73** arose from protosteryl cation (**5**) through from depronation C-17 without any hydride and methyl group shifts (**Scheme 33**). The characteristic *Z* configuration of $\Delta^{17(20)}$ that is found among fusidanes indicates that the side-chain moiety is folded in such a way that it does not require a substantial bond rotation between C-17 and C-20. This side-chain geometry is presumably conserved in lanosterol and cycloartenol synthases, as they all share 20*R* stereochemistry that can be achieved by a hydride migration from the α-face of C-17 without a significant bond rotation. This OSC gene was found clustered with eight other genes in the *A. fumigatus* genome, which includes genes for cytochrome P450 and short-chain dehydrogenase/reductase (SDR), which are presumed to be involved in the biosynthesis of helvolic acid (**74**). Fusidanes are clinically used antibiotics effective against Gram-positive bacteria such as *Staphylococcus aureus*.

1.18.4.4.6 Squalene cyclases from ferns

Ferns are known to produce a variety of triterpenes that lack C-3 oxygen functionality including hopanoids and migrated hopanoids. These triterpenes are believed to be derived from a cyclization of squalene. Therefore, ferns are expected to contain many squalene cyclase (SC) genes. The first SC gene from a fern *A. capillus-veneris* was identified and found to produce hopanol (**75**) as the sole product (**Scheme 34**).[44] This was in sharp contrast with bacterial SCs, which usually produce a mixture of hopene (**76**) and hopanol (**75**) in various ratios (Chapter 1.19). A cycloartenol synthase gene was also cloned from this fern, demonstrating that ferns contain both SC and OSC. Another SC gene was identified from *Dryopteris crassirhizoma* that produced dammara-18(28),21-diene (**78**).[100] This is the first demonstration of an SC that produces triterpene other than hopanoids. The dammarane-type triterpene **78** arose from C-3 deoxy dammarenyl cation **77** by a deprotonation from C-28 (**Scheme 35**). This SC exhibited 66% sequence identity with the one cloned from *A. capillus-veneris*. The fern SC sequences formed a distinct clade in the phylogenetic tree away from the bacterial sequences, indicating an independent evolution in the fern lineage.

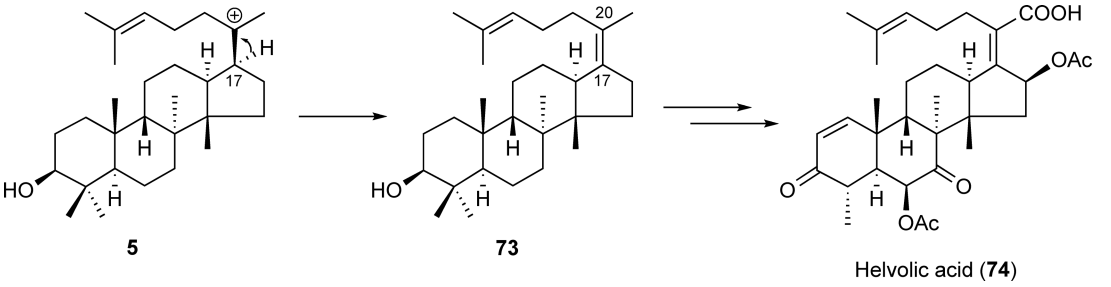

Scheme 33

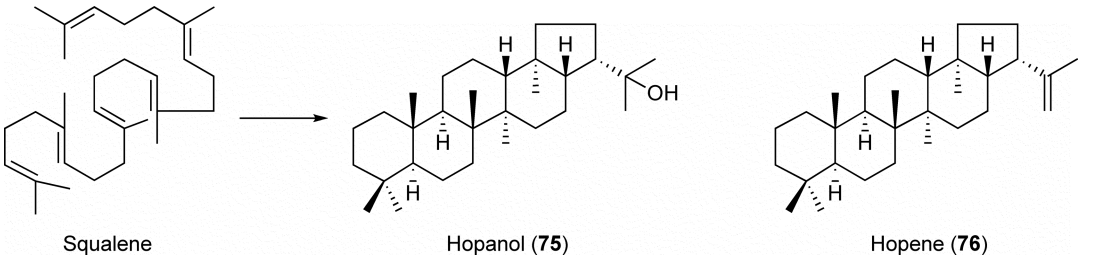

Scheme 34

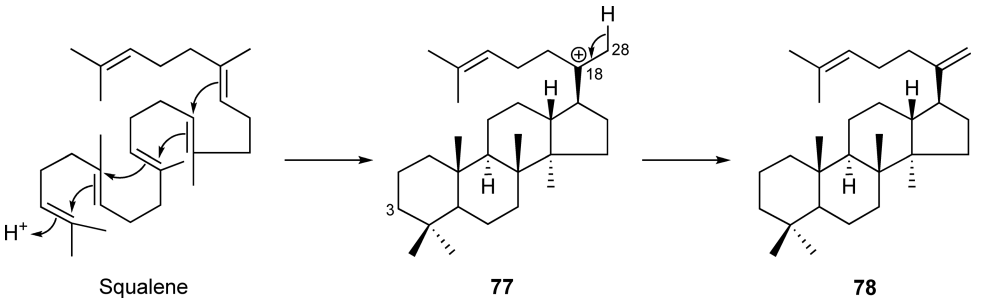

Squalene 77 78

Scheme 35

1.18.5 Triterpene Tailoring Steps

The formation of mature biologically active triterpenoids involves further modification of triterpene skeletons generated by OSCs, including an oxidation and a glycosylation. Triterpene saponins are found in many pharmaceutically important medicinal plants and exhibit rich biological activities. Despite extensive studies on OSCs, only a few limited studies are available for triterpene tailoring steps. Triterpene oxidation is generally thought to be catalyzed by cytochrome P450 monooxygenases (P450s).

The first P450 catalyzing the oxygenation of a triterpene substrate was identified from *G. max*, CYP93E1.[101] This P450 catalyzed a hydroxylation at C-24 of β-amyrin (**29**) and sophoradiol (**79**) to produce olean-12-ene-3β,24-diol (**80**) and soyasapogenol B (**81**), respectively (**Scheme 36**). This CYP93E1 is responsible for the soyasaponin biosynthesis in *G. max*. Soyasaponins, such as soyasaponin I (**82**) and soyasapogenol B, are known to possess strong hepatoprotective activity.

A second P450 gene that catalyzes triterpene oxygenation was identified from *G. uralensis*, CYP88D6.[102] This P450 catalyzed an oxygenation at C-11 of β-amyrin (**29**) to produce 11-oxo-β-amyrin (**84**) through 11α-hydroxy-β-amyrin (**83**) (**Scheme 37**). The two-step oxygenation that gives the 11-keto functionality is a characteristic step toward the biosynthesis of glycyrrhizin (**85**), a natural sweet compound that which possesses anti-inflammatory, immunomodulatory, antiulcer, antiallergy, and antiviral activities.

Fungal genes that modify protosta-17(20)*Z*,24-dien-3β-ol (**73**) were identified in the presumed helvolic acid biosynthetic gene cluster from *A. fumigatus*. A P450, CYP5081A1, was shown to catalyze the oxygenation of the 4β-methyl group to produce a diol (**86**) and a carboxylic acid (**87**) derivative (**Scheme 38**).[99] Another gene in the cluster that codes for an SDR was found to catalyze a dehydrogenation of the 3β-hydroxyl group of **73** to produce a 3-keto derivative (**88**).[99] These genes presumably function together to catalyze the demethylation of the 4β-methyl group during helvolic acid biosynthesis.

In oat *A. strigosa*, a P450 gene CYP51H10 was implicated as being involved in the biosynthesis of oleanane-type antifungal triterpene saponins, avenacins.[103] Mutation of this gene in oat resulted in a saponin-deficient phenotype. Therefore, CYP51H10 is expected to function in some oxidative modification steps of β-amyrin; however, the exact function of this gene remains to be studied.

In *A. thaliana*, two P450 genes were implicated as being involved in a triterpene tailoring reaction. In the vicinity of an OSC gene At5g48010 (thalianol synthase) in the genome, two P450 genes (CYP708A2 and CYP705A5) were found whose expression patterns were similar to the OSC gene. Both inactivation and overexpression studies of these genes resulted in accumulation of peaks on GC–MS, which were suggested to be thalianol (**46**) derivatives.[104] The exact function of these P450s also remains to be studied.

A glycosyltransferase gene responsible for a triterpene saponin biosynthesis was identified from *S. vaccaria*.[64] The plant family I glycosyltransferase, UGT74M1, was found to catalyze the attachment of glucose from uridine 5′-diphosphate-glucose (UDP-glucose) onto C-28 carboxylic acid of gypsogenic acid (**89**) to produce monoglucoside (**90**) (**Scheme 39**). This glycosyltransferase is presumably involved in the biosynthesis of the saponin vaccaroside B found in this plant.

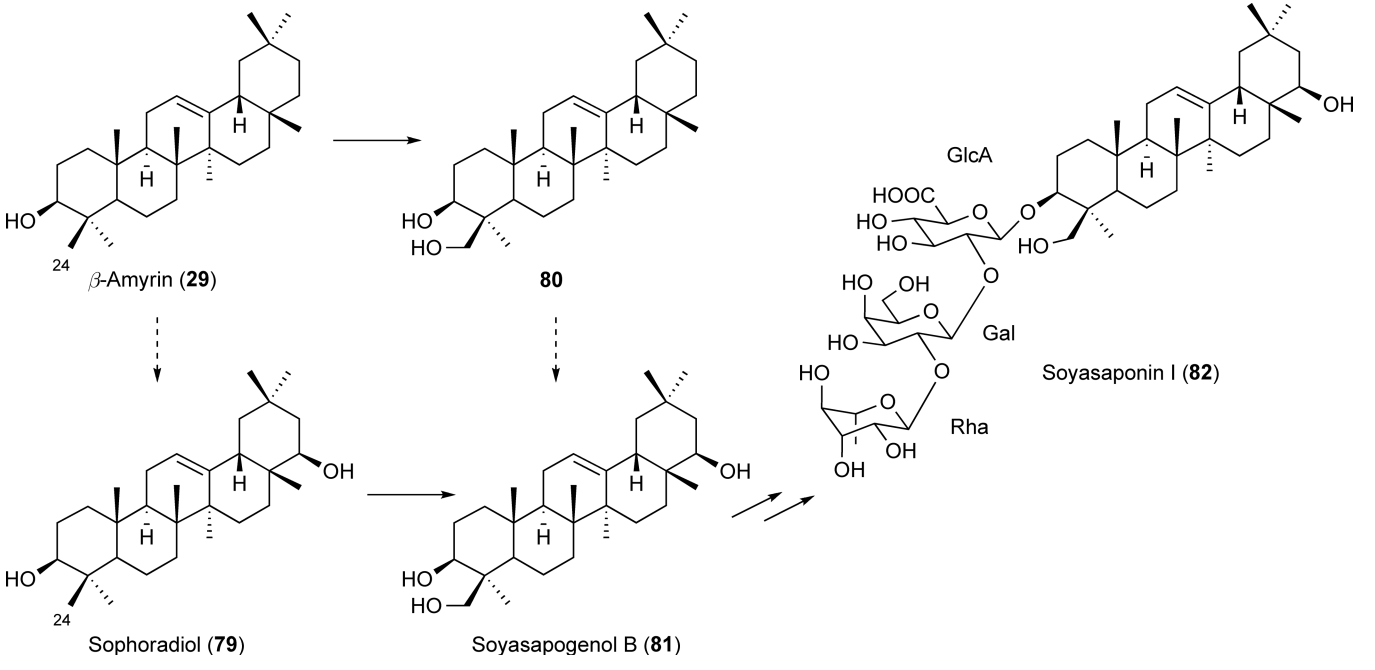
HO
24
β-Amyrin (29)
80
OH
Sophoradiol (79)
Soyasapogenol B (81)
GlcA
HOOC
Gal
Rha
Soyasaponin I (82)

Scheme 36

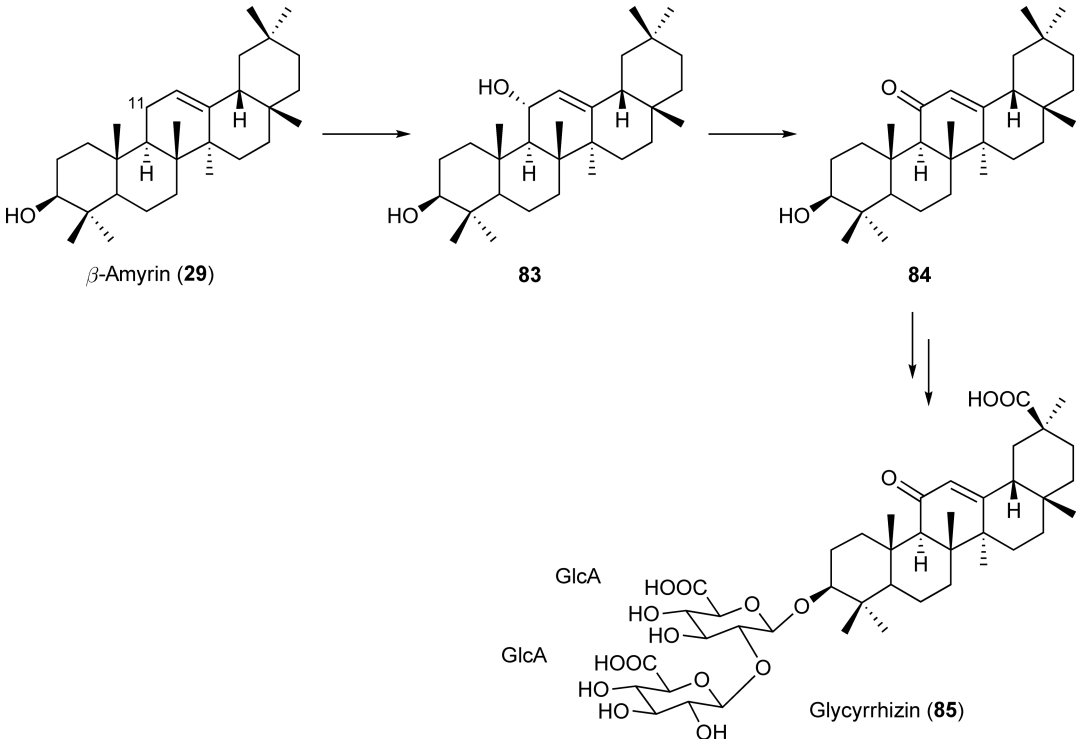

Scheme 37

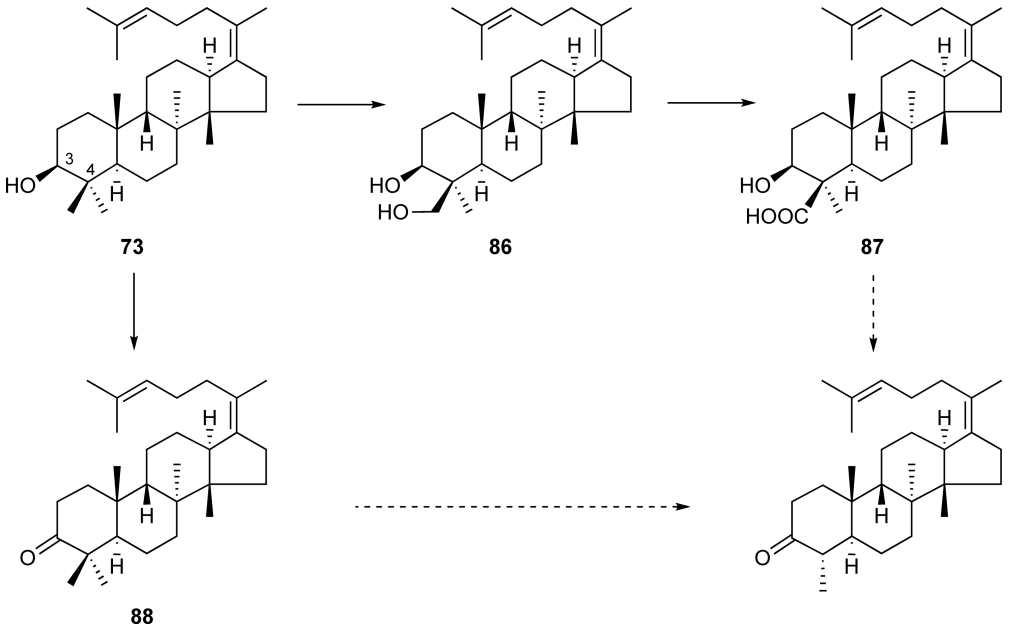

Scheme 38

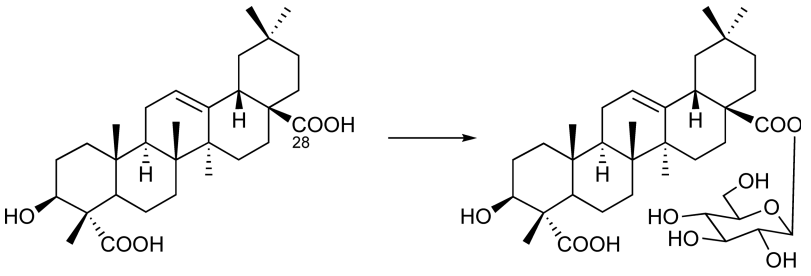

Gypsogenic acid (**89**) **90**

Scheme 39

1.18.6 Summary and Future Perspectives

The cyclization of oxidosqualene into various triterpenes has fascinated chemists for more than 60 years due to its remarkable chemistry and its ability to produce hundreds of different products from a single precursor. In recent years, significant progress in our understanding of the enzyme OSC has been made. These studies have uncovered the chemistry, enzymology, and genetics of OSCs to reveal the molecular mechanism of the catalysis and their biological roles in the cells. Notably, the first crystal structure of human lanosterol synthase has allowed us to observe the detailed structure of the active site. In addition, cloning of various plant OSC genes has revealed the existence of both product-specific and multifunctional OSCs in plants, which accounts for the generation of significant numbers of triterpene carbon skeletons found in nature. Our further understanding of such triterpene biosynthesis requires us to provide a detailed structural analysis of plant OSCs and to identify critical residues governing their product specificity. In this line, further cloning of OSC genes responsible for triterpenes that arise from mechanistically novel pathways would be valuable. Such triterpenes include friedelin (**91**), shionone (**92**), and onocerin (**94**). Friedelin (**91**) and shionone (**92**) arise from an oleanyl cation (**28**) and a baccharenyl cation (**24**), respectively, from extensive methyl and hydride shifts all the way up to C-3 without intervention by deprotonation; they are terminated with a ketone formation (**Scheme 40**). Studies on

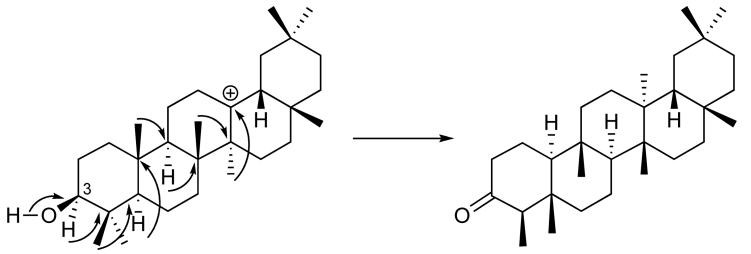

28 Friedelin (**91**)

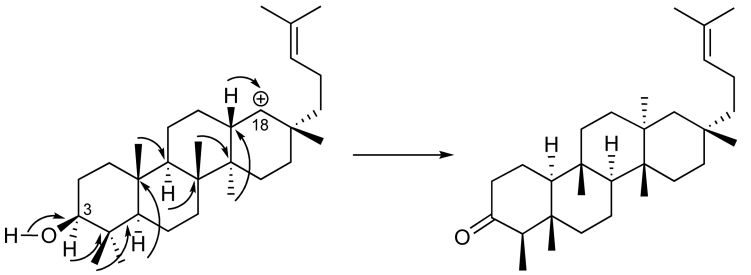

24 Shionone (**92**)

Scheme 40

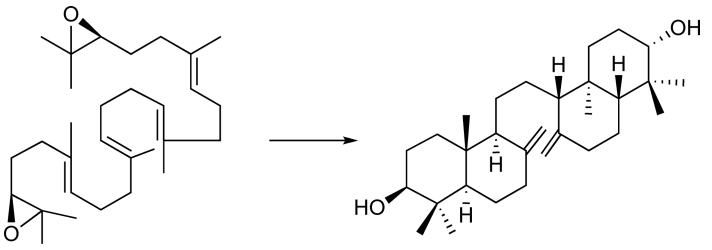

93 Onocerin (**94**)

Scheme 41

these OSCs would give us further insights into mechanisms that control Wagner–Meerwein shifts. On the other hand, onocerin (**94**) presumably arises from 2,3,22,23-dioxidosqualene (**93**) cyclized from both ends producing a bicyclic structure each (**Scheme 41**). Whether such products arise within a single active site or require the release of a singly cyclized product and recapture for another second round of cyclization is intriguing. In addition, triterpene tailoring steps are important for modifying triterpene skeletons to exhibit various biological activities. Currently, only a few limited studies are available for such triterpene tailoring steps. Identification of more genes involved in oxygenation and glycosylation is necessary for future engineering of triterpene biosynthesis to produce useful bioactive triterpenes.

Abbreviations

29-MOS	29-methylidene-2,3-oxidosqualene
BOS	baccharis oxide synthase
FPP	farnesyl diphosphate
IMS	isomultiflorenol synthase
OSC	oxidosqualene cyclase
P450	cytochrome P450 monooxygenase
SC	squalene cyclase
SDR	short-chain dehydrogenase/reductase
SHC	squalene:hopene cyclase

References

1. I. Shechter; G. Guan, *Comprehensive Natural Products Chemistry*; Elsevier: Oxford, 1999; Vol. 2, Chapter 9, pp 245–266.
2. I. Abe; G. D. Prestwich, *Comprehensive Natural Products Chemistry*; Elsevier: Oxford, 1999; Vol. 2, Chapter 10, pp 267–298.
3. A. Eschenmoser; D. Arigoni, *Helv. Chim. Acta* **2005**, *88*, 3011.
4. I. Abe; M. Rohmer; G. D. Prestwich, *Chem. Rev.* **1993**, *93*, 2189.
5. D. W. Christianson, *Chem. Rev.* **2006**, *106*, 3412.
6. R. Rajamani; J. Gao, *J. Am. Chem. Soc.* **2003**, *125*, 12768.
7. R. Xu; G. C. Fazio; S. P. T. Matsuda, *Phytochemistry* **2004**, *65*, 261.
8. E. J. Corey; H. Cheng; C. H. Baker; S. P. T. Matsuda; D. Li; X. Song, *J. Am. Chem. Soc.* **1997**, *119*, 1277.
9. E. J. Corey; S. C. Virgil; H. Cheng; C. H. Baker; S. P. T. Matsuda; V. Singh; S. Sarshar, *J. Am. Chem. Soc.* **1995**, *117*, 11819.
10. E. J. Corey; S. C. Virgil, *J. Am. Chem. Soc.* **1991**, *113*, 4025.
11. E. J. Corey; S. C. Virgil; D. R. Liu; S. Sarshar, *J. Am. Chem. Soc.* **1992**, *114*, 1524.
12. R. Kelly; S. M. Miller; M. H. Lai; D. R. Kirsch, *Gene* **1990**, *87*, 177.
13. C. J. Buntel; J. H. Griffin, *J. Am. Chem. Soc.* **1992**, *114*, 9711.
14. C. A. Roessner; C. Min; S. H. Hardin; L. W. Harris-Haller; J. C. McCollum; A. I. Scott, *Gene* **1993**, *127*, 149.
15. E. J. Corey; S. P. T. Matsuda; B. Bartel, *Proc. Natl. Acad. Sci. U.S.A.* **1994**, *91*, 2211.
16. Z. Shi; C. J. Buntel; J. H. Griffin, *Proc. Natl. Acad. Sci. U.S.A.* **1994**, *91*, 7370.
17. E. J. Corey; S. P. T. Matusda; C. H. Baker; A. Y. Ting; H. Cheng, *Biochem. Biophys. Res. Commun.* **1996**, *219*, 327.
18. M. Kusano; M. Shibuya; U. Sankawa; Y. Ebizuka, *Biol. Pharm. Bull.* **1995**, *18*, 195.

19. I. Abe; G. D. Prestwich, *Proc. Natl. Acad. Sci. U.S.A.* **1995**, *92*, 9274.
20. C. K. Sung; M. Shibuya; U. Sankawa; Y. Ebizuka, *Biol. Pharm. Bull.* **1995**, *18*, 1459.
21. C. H. Baker; S. P. T. Matsuda; D. R. Liu; E. J. Corey, *Biochem. Biophys. Res. Commun.* **1995**, *213*, 154.
22. K. Poralla; A. Hewelt; G. D. Prestwich; I. Abe; I. Reipen; G. Sprenger, *Trends Biochem. Sci.* **1994**, *19*, 157.
23. K. Poralla, *Bioorg. Med. Chem. Lett.* **1994**, *4*, 285.
24. R. Thoma; T. Schulz-Gasch; B. D'Arcy; J. Benz; J. Aebi; H. Dehmlow; M. Hennig; M. Stihle; A. Ruf, *Nature* **2004**, *432*, 118.
25. F. S. Buckner; L. N. Ngyuen; B. M. Joubert; S. P. T. Matsuda, *Mol. Biochem. Parasitol.* **2000**, *110*, 399.
26. B. M. Joubert; F. S. Buckner; S. P. T. Matsuda, *Org. Lett.* **2001**, *3*, 1957.
27. I. Abe; K. Naito; Y. Takagi; H. Noguchi, *Biochim. Biophys. Acta* **2001**, *1522*, 67.
28. P. Milla; F. Viola; S. Oliaro-Bosso; F. Rocco; L. Cattel; B. M. Joubert; R. J. LeClair; S. P. T. Matsuda; G. Balliano, *Lipids* **2002**, *37*, 1171.
29. M. D. Kolesnikova; Q. Xiong; S. Lodeiro; L. Hua; S. P. T. Matsuda, *Arch. Biochem. Biophys.* **2006**, *447*, 87.
30. M. Suzuki; T. Xiang; K. Ohyama; H. Seki; K. Saito; T. Muranaka; H. Hayashi; Y. Katsube; T. Kushiro; M. Shibuya; Y. Ebizuka, *Plant Cell Physiol.* **2006**, *47*, 565.
31. S. Sawai; T. Akashi; N. Sakurai; H. Suzuki; D. Shibata; S. Ayabe; T. Aoki, *Plant Cell Physiol.* **2006**, *47*, 673.
32. E. J. Corey; S. P. T. Matsuda; B. Bartel, *Proc. Natl. Acad. Sci. U.S.A.* **1993**, *90*, 11628.
33. M. Morita; M. Shibuya; M.-S. Lee; U. Sankawa; Y. Ebizuka, *Biol. Pharm. Bull.* **1997**, *20*, 770.
34. T. Kushiro; M. Shibuya; Y. Ebizuka, *Eur. J. Biochem.* **1998**, *256*, 238.
35. H. Hayashi; N. Hiraoka; Y. Ikeshiro; K. Yazaki; S. Tanaka; T. Kushiro; M. Shibuya; Y. Ebizuka, *Plant Physiol.* **1999**, *121*, 1384.
36. S. M. Godzina; M. A. Lovato; M. M. Meyer; K. A. Foster; W. K. Wilson; W. Gu; E. L. de Hostos; S. P. T. Matsuda, *Lipids* **2000**, *35*, 249.
37. H. Hayashi; N. Hiraoka; Y. Ikeshiro; T. Kushiro; M. Morita; M. Shibuya; Y. Ebizuka, *Biol. Pharm. Bull.* **2000**, *23*, 231.
38. N. Kawano; K. Ichinose; Y. Ebizuka, *Biol. Pharm. Bull.* **2002**, *25*, 477.
39. H. Zhang; M. Shibuya; S. Yokota; Y. Ebizuka, *Biol. Pharm. Bull.* **2003**, *26*, 642.
40. M. Shibuya; S. Adachi; Y. Ebizuka, *Tetrahedron* **2004**, *60*, 6995.
41. O. Guhling; B. Hobl; T. Yeats; R. Jetter, *Arch. Biochem. Biophys.* **2006**, *448*, 60.
42. S. Sawai; T. Shindo; S. Sato; T. Kaneko; S. Tabata; S. Ayabe; T. Aoki, *Plant Sci.* **2006**, *170*, 247.
43. M. Basyuni; H. Oku; E. Tsujimoto; S. Baba, *Biosci. Biotechnol. Biochem.* **2007**, *71*, 1788.
44. J. Shinozaki; M. Shibuya; K. Masuda; Y. Ebizuka, *FEBS Lett.* **2008**, *582*, 310.
45. D. C. Lamb; C. J. Jackson; A. G. S. Warrilow; N. J. Manning; D. E. Kelly; S. L. Kelly, *Mol. Biol. Evol.* **2007**, *24*, 1714.
46. C. Nakano; A. Motegi; T. Sato; M. Onodera; T. Hoshino, *Biosci. Biotechnol. Biochem.* **2007**, *71*, 2543.
47. H. B. Bode; B. Zeggel; B. Silakowski; S. C. Wenzel; H. Reichenbach; R. Müller, *Mol. Microbiol.* **2003**, *47*, 471.
48. I. Abe; G. D. Prestwich, *J. Biol. Chem.* **1994**, *269*, 802.
49. E. J. Corey; H. Cheng; C. H. Baker; S. P. T. Matsuda; D. Li; X. Song, *J. Am. Chem. Soc.* **1997**, *119*, 1289.
50. E. A. Hart; L. Hua; L. B. Darr; W. K. Wilson; J. Pang; S. P. T. Matsuda, *J. Am. Chem. Soc.* **1999**, *121*, 9887.
51. B. M. Joubert; L. Hua; S. P. T. Matsuda, *Org. Lett.* **2000**, *2*, 339.
52. S. P. T. Matsuda; L. B. Darr; E. A. Hart; J. B. R. Herrera; K. E. McCann; M. M. Meyer; J. Pang; H. G. Schepmann, *Org. Lett.* **2000**, *2*, 2261.
53. M. J. R. Segura; B. E. Jackson; S. P. T. Matsuda, *Nat. Prod. Rep.* **2003**, *20*, 304.
54. I. Abe, *Nat. Prod. Rep.* **2007**, *24*, 1311.
55. T. K. Wu; C. H. Chang; Y. T. Liu; T. T. Wang, *Chem. Rec.* **2008**, *8*, 302.
56. S. Lodeiro; T. Schulz-Gasch; S. P. T. Matsuda, *J. Am. Chem. Soc.* **2005**, *127*, 14132.
57. J. B. R. Herrera; B. Bartel; W. K. Wilson; S. P. T. Matsuda, *Phytochemistry* **1998**, *49*, 1905.
58. M. Morita; M. Shibuya; T. Kushiro; K. Masuda; Y. Ebizuka, *Eur. J. Biochem.* **2000**, *267*, 3453.
59. H. Hayashi; P. Huang; A. Kirakosyan; K. Inoue; N. Hiraoka; Y. Ikeshiro; T. Kushiro; M. Shibuya; Y. Ebizuka, *Biol. Pharm. Bull.* **2001**, *24*, 912.
60. K. Haralampidis; G. Bryan; X. Qi; K. Papadopoulou; S. Bakht; R. Melton; A. Osbourn, *Proc. Natl. Acad. Sci. U.S.A.* **2001**, *98*, 13431.
61. H. Suzuki; L. Achnine; R. Xu; S. P. T. Matsuda; R. A. Dixon, *Plant J.* **2002**, *32*, 1033.
62. I. Iturbe-Ormaetxe; K. Haralampidis; K. Papadopoulou; A. E. Osbourn, *Plant Mol. Biol.* **2003**, *51*, 731.
63. M. Kajikawa; K. T. Yamato; H. Fukuzawa; Y. Sakai; H. Uchida; K. Ohyama, *Phytochemistry* **2005**, *66*, 1759.
64. D. Meesapyodsuk; J. Balsevich; D. W. Reed; P. S. Covello, *Plant Physiol.* **2007**, *143*, 959.
65. M. Basyuni; H. Oku; E. Tsujimoto; K. Kinjo; S. Baba; K. Takara, *FEBS J.* **2007**, *274*, 5028.
66. J. Kirby; D. W. Romanini; E. M. Paradise; J. D. Keasling, *FEBS J.* **2008**, *275*, 1852.
67. M. Cammareri; M. F. Consiglio; P. Pecchia; G. Corea; V. Lanzotti; J. I. Ibeas; A. Tava; C. Conicella, *Plant Sci.* **2008**, *175*, 255.
68. M. Shibuya; Y. Katsube; M. Otsuka; H. Zhang; P. Tansakul; T. Xiang; Y. Ebizuka, *Plant Physiol. Biochem.* **2009**, *47*, 26.
69. M. J. R. Segura; M. M. Meyer; S. P. T. Matsuda, *Org. Lett.* **2000**, *2*, 2257.
70. M. Shibuya; H. Zhang; A. Endo; K. Shishikura; T. Kushiro; Y. Ebizuka, *Eur. J. Biochem.* **1999**, *266*, 302.
71. H. Hayashi; P. Huang; S. Takada; M. Obinata; K. Inoue; M. Shibuya; Y. Ebizuka, *Biol. Pharm. Bull.* **2004**, *27*, 1086.
72. T. Kushiro; M. Shibuya; Y. Ebizuka, *J. Am. Chem. Soc.* **1999**, *121*, 1208.
73. T. Kushiro; M. Shibuya; Y. Ebizuka, *Tetrahedron Lett.* **1999**, *40*, 5553.
74. T. Kushiro; M. Hoshino; T. Tsutsumi; K. Kawai; M. Shiro; M. Shibuya; Y. Ebizuka, *Org. Lett.* **2006**, *8*, 5589.
75. T. Kushiro; M. Shibuya; K. Masuda; Y. Ebizuka, *J. Am. Chem. Soc.* **2000**, *122*, 6816.
76. M. Basyuni; H. Oku; M. Inafuku; S. Baba; H. Iwasaki; K. Oshiro; T. Okabe; M. Shibuya; Y. Ebizuka, *Phytochemistry* **2006**, *67*, 2517.
77. H. Saimaru; Y. Orihara; P. Tansakul; Y. H. Kang; M. Shibuya; Y. Ebizuka, *Chem. Pharm. Bull.* **2007**, *55*, 784.
78. E. Babiychuk; P. Bouvier-Navé; V. Compagnon; M. Suzuki; T. Muranaka; M. Van Montagu; S. Kushnir; H. Schaller, *Proc. Natl. Acad. Sci. U.S.A.* **2008**, *105*, 3163.
79. T. Kushiro; M. Shibuya; K. Masuda; Y. Ebizuka, *Tetrahedron Lett.* **2000**, *41*, 7705.

80. M. D. Kolesnikova; W. K. Wilson; D. A. Lynch; A. C. Obermeyer; S. P. T. Matsuda, *Org. Lett.* **2007**, *9*, 5223.
81. Y. Ebizuka; Y. Katsube; T. Tsutsumi; T. Kushiro; M. Shibuya, *Pure Appl. Chem.* **2003**, *75*, 369.
82. G. C. Fazio; R. Xu; S. P. T. Matsuda, *J. Am. Chem. Soc.* **2004**, *126*, 5678.
83. T. Xiang; M. Shibuya; Y. Katsube; T. Tsutsumi; M. Otsuka; H. Zhang; K. Masuda; Y. Ebizuka, *Org. Lett.* **2006**, *8*, 2835.
84. M. D. Kolesnikova; A. C. Obermeyer; W. K. Wilson; D. A. Lynch; Q. Xiong; S. P. T. Matsuda, *Org. Lett.* **2007**, *9*, 2183.
85. K. Ohyama; M. Suzuki; J. Kikuchi; K. Saito; T. Muranaka, *Proc. Natl. Acad. Sci. U.S.A.* **2009**, *106*, 725.
86. Q. Xiong; W. K. Wilson; S. P. T. Matsuda, *Angew. Chem. Int. Ed.* **2006**, *45*, 1285.
87. M. Shibuya; T. Xiang; Y. Katsube; M. Otsuka; H. Zhang; Y. Ebizuka, *J. Am. Chem. Soc.* **2007**, *129*, 1450.
88. T. Akihisa; K. Koike; Y. Kimura; N. Sashida; T. Matsumoto; M. Ukiya; T. Nikaido, *Lipids* **1999**, *34*, 1151.
89. T. Akihisa; Y. Kimura; K. Koike; T. Shibata; Z. Yoshida; T. Nikaido; T. Tamura, *J. Nat. Prod.* **1998**, *61*, 409.
90. T. Akihisa; K. Yasukawa; Y. Kimura; S. Yamanouchi; T. Tamura, *Phytochemistry* **1998**, *48*, 301.
91. T. Akihisa; K. Arai; Y. Kimura; K. Koike; W. C. M. C. Kokke; T. Shibata; T. Nikaido, *J. Nat. Prod.* **1999**, *62*, 265.
92. S. Lodeiro; Q. Xiong; W. K. Wilson; M. D. Kolesnikova; C. S. Onak; S. P. T. Matsuda, *J. Am. Chem. Soc.* **2007**, *129*, 11213.
93. H. Hayashi; P. Huang; K. Inoue; N. Hiraoka; Y. Ikeshiro; K. Yazaki; S. Tanaka; T. Kushiro; M. Shibuya; Y. Ebizuka, *Eur. J. Biochem.* **2001**, *268*, 6311.
94. T. Kushiro; Y. Ohno; M. Shibuya; Y. Ebizuka, *Biol. Pharm. Bull.* **1997**, *20*, 292.
95. S. Shibata; O. Tanaka; J. Shoji; H. Saito, *Economic and Medicinal Plant Research*; Academic Press: London, 1985; Vol. 1, p 217.
96. P. Tansakul; M. Shibuya; T. Kushiro; Y. Ebizuka, *FEBS Lett.* **2006**, *580*, 5143.
97. J. D. White; J. Fayos; J. Clardy, *J. Chem. Soc. Chem. Commun.* **1973**, 357.
98. M. Shibuya; A. Sagara; A. Saitoh; T. Kushiro; Y. Ebizuka, *Org. Lett.* **2008**, *10*, 5071.
99. H. Mitsuguchi; Y. Seshime; I. Fujii; M. Shibuya; Y. Ebizuka; T. Kushiro, *J. Am. Chem. Soc.* **2009**, *131*, 6402.
100. J. Shinozaki; M. Shibuya; K. Masuda; Y. Ebizuka, *Phytochemistry* **2008**, *69*, 2559.
101. M. Shibuya; M. Hoshino; Y. Katsube; H. Hayashi; T. Kushiro; Y. Ebizuka, *FEBS J.* **2006**, *273*, 948.
102. H. Seki; K. Ohyama; S. Sawai; M. Mizutani; T. Ohnishi; H. Sudo; T. Akashi; T. Aoki; K. Saito; T. Muranaka, *Proc. Natl. Acad. Sci. U.S.A.* **2008**, *105*, 14204.
103. X. Qi; S. Bakht; B. Qin; M. Leggett; A. Hemmings; F. Mellon; J. Eagles; D. Werck-Reichhart; H. Schaller; A. Lesot; R. Melton; A. Osbourn, *Proc. Natl. Acad. Sci. U.S.A.* **2006**, *103*, 18848.
104. B. Field; A. E. Osbourn, *Science* **2008**, *320*, 543.

Biographical Sketches

Tetsuo Kushiro received his B.S. in chemistry from the Tokyo Institute of Technology (1993) and Ph.D. from the Graduate School of Pharmaceutical Sciences, The University of Tokyo (1998), where he studied with Professor Yutaka Ebizuka. He carried out JSPS postdoctoral research at the same laboratory (1998–2000) and then at The Scripps Research Institute with Professor Paul Schimmel (2000–02). He became research associate at Plant Science Center, RIKEN Institute, working with Dr. Yuji Kamiya (2002–05). He was then appointed assistant professor at The University of Tokyo in 2005. His current research includes biosynthesis of terpenoids in both plants and fungi, especially triterpenoids and meroterpenoids.

Yutaka Ebizuka is a Professor at the Graduate School of Pharmaceutical Sciences, The University of Tokyo in Japan. He received his Ph.D. from the Graduate School of Pharmaceutical Sciences, The University of Tokyo in 1974. After 2-year postdoctoral experience in Department of Chemistry and Department of Botany at the University of British Columbia in Vancouver, he returned to The University of Tokyo as an assistant professor. He has been Professor of Natural Products Chemistry since 1995. He has received several distinctions, which include the awards from the Japanese Society for Plant Cell and Molecular Biology (2001), Japanese Society of Pharmacognosy (2006), and the Pharmaceutical Society of Japan (2007). His research interests include biosynthetic studies of natural products from polyketide and terpenoid pathways.